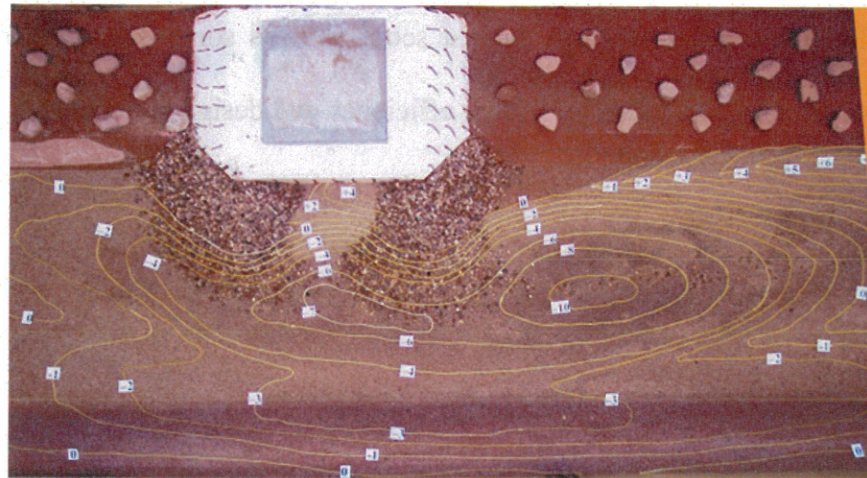
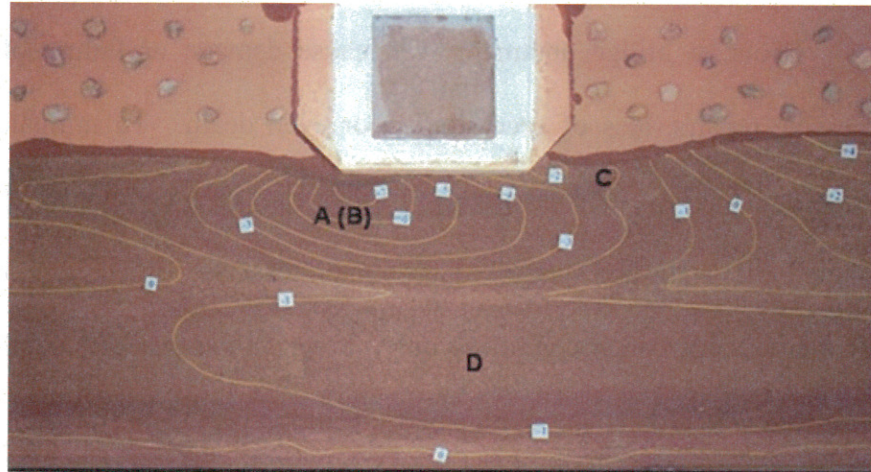


COUNTERMEASURES AGAINST SCOUR AT ABUTMENTS



Hua Li, Roger A. Kuhnle, Brian D. Barkdoll

Channel and Watershed Processes Research Unit
National Sedimentation Laboratory
USDA Agricultural Research Service
Oxford, Mississippi 38655

LIBRARY
USDA ARS MSA
National Sedimentation Laboratory
P.O. Box 1167, Oxford, MS 38655

Research Report No. 49

January, 2006

TABLE OF CONTENTS

LIST OF FIGURES

LIST OF TABLES

LIST OF SYMBOLS

CHAPTER 1. INTRODUCTION

1.1 Introduction.....	1-1
1.2 Scope of study.....	1-2

CHAPTER 2. A LITERATURE REVIEW ON BRIDGE ABUTMENT SCOUR

2.1 Introduction.....	2-1
2.2 Bridge Abutment Scour Mechanism.....	2-1
2.3 Parameters Influencing Local Scour at Abutments.....	2-3
2.3.1 Time Evolution.....	2-3
2.3.2 The Effect of Flow Velocity.....	2-6
2.3.3 The Effect of Flow Depth.....	2-8
2.3.4 The Effect of Sediment Size	2-8
2.3.5 The Effect of Sediment Gradation.....	2-10
2.3.6 The effect of abutment length.....	2-11
2.3.7 The Effect of Abutment Shape.....	2-13
2.3.8 The Effect of Abutment Skewness.....	2-15
2.3.9 The Effect of Approach Channel Geometry.....	2-16
2.3.10 Experimental studies of scour at abutment in compound channels.....	2-19

CHAPTER 3. A LITERATURE REVIEW ON BRIDGE ABUTMENT SCOUR COUNTERMEASURES

3.1 Introduction.....	3-1
3.2 Spurs dikes.....	3-1
3.2.1 Introduction.....	3-1
3.2.2 Local Scour at Spur Dikes.....	3-4
3.2.3 Empirical Formulas.....	3-9
3.2.4 Semi-analytical and Analytical Formulae.....	3-14
3.2.5 Numerical Simulations around Spur-dikes.....	3-15
3.2.6 Design Considerations for Spur Dike Systems.....	3-18
3.2.6.1 Length and Spacing of Spur Dikes.....	3-18
3.2.6.2 Orientation of Spur Dikes.....	3-20
3.2.6.3 Permeability.....	3-23
3.2.6.4 Spur Height, Crest Profile, and Spur Head Form.....	3-25
3.2.6.5 Other Design Considerations.....	3-27
3.2.7 Application of Spur dikes.....	3-27
3.3 Hardpoints	3-28
3.4 Guide banks.....	3-29

6.4.1 Protrusion of Wall.....	6-17
6.4.2 Length of Wall.....	6-18
6.4.3 Height and Width of Wall Crest.....	6-18
6.4.4 Slope of Wall and Apron	6-18
6.4.5 Comparison of Solid and Rock Parallel Walls.....	6-19
6.5 Conclusions.....	6-19

CHAPTER 7. SPUR DIKE AS AN ABUTMENT SCOUR COUNTERMEASURE

7.1 Introduction.....	7-1
7.2 Conceptual Model.....	7-3
7.3 Results.....	7-4
7.3.1 Solid Spur Dikes.....	7-4
7.3.2 Rock Spur Dikes.....	7-7
7.4 Design of Spur Dikes for Scour Prevention at Wing-wall Abutments.....	7-15
7.5 Conclusions.....	7-17

CHAPTER 8. BRIDGE ABUTMENT COLLAR AS A SCOUR COUNTERMEASURE

8.1 Introduction.....	8-1
8.2 Conceptual Model.....	8-1
8.3 Collar Results.....	8-2
8.4 Discussion.....	8-4
8.4.1 Protrusion Width	8-4
8.4.2 Collar Elevation.....	8-6
8.4.3 Streamwise Collar Length	8-6
8.4.4 Temporal Scour Variation.....	8-8
8.5 Conclusions.....	8-8

CHAPTER 9. SUMMARY

9.1 Summary.....	9-1
9.2 Limitation of Study.....	9-2
9.3 Future Work.....	9-3

REFERENCES

Fig. 6-5: Scour contours of test No 3. in Table 6-3 with gravel diameter 6.7~9.5 mm, 1.5L length, rock wall end slope H:V=30/13.2, side slope H:V=18/13.2, a small apron at the end . Wall base protruded out into main channel from abutment half wall width. $y_m = 13.2$ cm, $y_f = 5.2$ cm, $Q = 0.0369$ m³/s, $t = 4800$ min. Flow from left to right.

Fig. 6-6: Scour contour of test No 6. in Table 4 with gravel diameter 6.7~9.5 mm, 1.5L length, rock wall end slope H:V=30/13.2, side slope H:V=18/13.2, a small apron at the end . Wall base protruded out into main channel from abutment a quarter wall width. $y_m = 13.2$ cm, $y_f = 5.2$ cm, $Q = 0.0373$ m³/s, $t = 4800$ min. Flow from left to right.

Fig. 6-7: Scour contour of Test 9. in Table 6-3 with gravel diameter 6.7~9.5 mm, 1.5L length, rock wall end slope H:V=30/13.2, side slope H:V=18/13.2, a small apron at the end . Wall base is even with abutment. $y_m = 13.2$ cm, $y_f = 5.2$ cm, $Q = 0.0371$ m³/s, $t = 4800$ min. Flow from left to right.

Fig. 6-8: Plot of scour depth at bridge abutment versus rock wall length for different wall protrusion lengths under clear-water conditions ($U/U_c=0.9$).

Fig. 6-9: Plot of the maximum scour depth caused by the wall in the entire channel versus rock wall length for different wall protrusion lengths under clear-water conditions ($U/U_c=0.9$).

Fig. 6-10: Plot of both time-averaged and maximum instantaneous scour depth at bridge abutment versus rock wall length for zero protrusion under live bed conditions, $U/U_c = 1.5$.

Fig. 7-1: Photograph of excessive scour around a poorly-positioned spur dike. (Flow from left to right.)

Figure 7-2: A sketch of the conceptual model of a spur dike as a countermeasure against abutment scour in a compound channel.

Fig. 7-3: Photograph of Sp-3. Flow from left to right.

Fig. 7-4: Photograph of Sp-5. Flow from left to right.

Fig. 7-5: Photograph of Sp-6. Flow from left to right.

Fig. 7-6: Scour contour of Test Sp-7 with two spur dikes upstream of the abutment. Flow was from left to right.

Fig. 7-7: Scour contour of Test Sp-8 with three spur dikes (including the two formed by the abutment). The flow was from left to right.

Fig. 7-8: Scour contour of Test Sp-9 with three spur dikes (including the one formed by the abutment). The flow was from left to right.

LIST OF TABLES

Table 2-1: Parameters influencing local scour at abutments.

Table 2-2: Shape factors

Table 3-1. Spur dike spacing recommendations.

Table 5-1. Baseline clear-water experimental results with $U/U_c=0.9$.

Table 5-2. Experimental results for baseline scour depth for three velocity ratios.

Table 6-1: Solid wall experimental results for clear-water scour (run time=4800 min., $Q=0.0379 \pm 0.003 \text{ m}^3/\text{s}$, $U/U_c=0.9$).

Table 6-2: Solid wall experimental results for live-bed scour (run time=3000 min., $Q=0.0619 \pm 0.0015 \text{ m}^3/\text{s}$ for $U/U_c=1.5$, and $Q=0.0619 \pm 0.0015 \text{ m}^3/\text{s}$ for $U/U_c=2.3$, all walls were rectangular shaped and emergent).

Table 6-3: Experimental data of parallel rock walls in clear-water scour ($Q = 0.0385 \pm 0.003 \text{ m}^3/\text{s}$, $t = 4800 \text{ min.}$, $U/U_c=0.9$).

Table 6-4: Rock wall experimental results in live-bed scour (run time=3000 min., $Q=0.0619 \pm 0.0015 \text{ m}^3/\text{s}$ for $U/U_c=1.5$, and $Q=0.0966 \pm 0.003 \text{ m}^3/\text{s}$ for $U/U_c=2.3$, all walls were rectangular shaped and emergent).

Table 6-5: Comparison of rock and solid wall countermeasure performance (scour depth (cm)).

Table 7-1: Preliminary Solid Spur Dike Experimental Results ($Q=0.0387 \pm 0.003 \text{ m}^3/\text{s}$, $U/U_c=0.9$, $y_m = 13.2 \text{ cm}$, $y_f=5.2 \text{ cm}$).

Table 7-2: Clear-water experimental data of rock spur dikes ($Q = 0.0368 \pm 0.0016 \text{ m}^3/\text{s}$, $U/U_c=0.9$, $y_m = 13.2 \text{ cm}$, $y_f=5.2 \text{ cm}$, gravel diameter $D = 6.7 \sim 9.5 \text{ mm}$, running time $t = 4800 \text{ min}$, all spur dikes had a top protrusion length of $1.0L_a$, a bottom protrusion length of $1.5L_a$, and end slope of $H:V=22/13.2$).

Table 7-3: Live-bed experimental data of rock spur dikes ($Q = 0.0627 \pm 0.003 \text{ m}^3/\text{s}$ for velocity ratio of 1.5 and 0.0985 for velocity ratio of 2.3, $y_m = 13.2 \text{ cm}$, $y_f=5.2 \text{ cm}$, running time $t = 3000 \text{ min}$).

Table 8-1. Dimensions and positions of collars tested (run time=4800 min., $y_m = 13.2 \text{ cm}$, $y_f = 5.2$, $Q=0.0387 \pm 0.001 \text{ m}^3/\text{s}$, $U/U_c=0.9$).

d_{50}	median particle size
$d_{84.1}$	particle size for which 84.1 percent of the sediment mixture is finer
$d_{15.9}$	particle size for which 15.9 percent is of the sediment mixture finer
\bar{d}_s	dimensionless maximum scour depth
D	distance or diameter of cylinder pier
D_r	rock size for guide banks
D_s	distance between two successive spur dikes or between spur dike and abutment
f	Lacey silt factor
F_n	Froude number
F_f	approach flow Froude number on the floodplain
F_{fc}	critical Froude number on the floodplain
F_{bo}	Blench's zero bed factor which is a function of grain size
g	gravitational constant
h_1	main channel bank height
k	function of approach conditions
$\kappa - \varepsilon$	viscous and turbulent
K	function of C_D which varies between 2.5 and 5.0
k_s	Nikuradse sand roughness coefficient
K_G	channel geometry factor
K_I	flow intensity factor
K_y	flow depth factor
K_d	sediment size factor

S_o	Slope of channel
S_s	specific gravity
S_p	particle shape factor
S_b	side slope of rock walls
S_n	end slope of rock walls
t	time
T	temperature
U	mean approach velocity
U_c	critical velocity
U_a	mean approach flow velocity at the armor peak
u^*	shear velocity
u^*_c	critical shear velocity
U_{ab}	the maximum resultant velocity at the upstream corner of the abutment face y_{ab}
	floodplain flow depth at the location of U_{ab} in the contracted section
Y_0	flow depth
y_s	depth of flow at abutment, i.e., $d_s + y_0$
y_f	mean flow depth on floodplain
y_{f0}	undisturbed average flow depth in the approach floodplain
y_m	flow depth in main channel
V_u	peak downflow velocity
V	transverse velocity
ν_t	kinematic viscosity due to turbulence
w	sediment fall velocity
W	effective bottom width of rock wall countermeasure
ϕ	angle of repose
ι	Prandtl mixing length
θ	angle of attack or abutment (spur dike) skewness
θ_1	Shields entrainment function
θ_c	critical Shields entrainment function
ρ	density of water

CHAPTER 1. INTRODUCTION

1.1 Introduction

Scour is the result of the erosive action of flowing water, excavating and carrying away material from the bed and banks of streams. Different materials scour at different rates. Loose granular soils are rapidly eroded under water action while cohesive or cemented soils are more scour-resistant. However, ultimate scour in cohesive or cemented soils can be as deep as scour in sand bed streams. Scour will reach its maximum depth in sand and gravel bed materials in hours; cohesive bed materials in days; glacial tills, poorly cemented sand stones and shales in months; hard dense and cemented sandstone or shales in years; and granites in centuries. Massive rock formations with few discontinuities can be highly resistant to scour and erosion during the lifetime of a typical bridge. Detailed discussion and equations for calculating all bridge scour components are presented in HEC-18 (Richardson and Davis, 1995).

Total scour at a highway crossing is comprised of the following three components: aggradation or degradation, contraction scour and local scour. Aggradation or degradation is long-term streambed elevation changes due to natural or human-induced causes within the reach of the river on which the bridge is located. Contraction scour involves the removal of material from the bed and banks across all or most of the width of the channel. This scour can result from a contraction of the flow by the approach embankments to the bridge encroaching onto the floodplain and/or into the main channel, from a change in downstream control of the water surface elevation, or from the location of the bridge in relation to a bend. In each case, scour is caused by an increase in transport of bed material in the bridge cross section. Local scour occurs around piers, abutments, spurs and embankments and is caused by the acceleration of the flow and the development of vortex systems induced by these obstructions to the flow.

Bridge failures due to total scour at bridge foundations (i.e., bridge abutments and piers) have prompted a heightened interest in scour prediction and scour countermeasures. Data showed that the problem of scouring at bridge abutments is quite significant.

The ultimate aim of this study of countermeasures against scour at bridge abutments is to determine design guidelines for those countermeasures that are efficient in preventing or reducing local scour at the abutments of small county bridges, and through which bridge abutments can be well protected. The prerequisite to such guidelines is obtaining normalizing parameters that collapse experimental data and adequately scale model study results to field situations. Countermeasures that will be investigated here include spur dikes, parallel walls, and collars. Since few countermeasures can totally eliminate scour for all of the complex situations that occur in natural rivers and for all of the various bridge configurations encountered, it becomes necessary that a goal of scour reduction be defined. For the purpose of this project, a primary goal is to identify countermeasures that reduce maximum local scour depth by 65 to 75 percent of the scour depth occurring at an unprotected abutment.

An extensive study is presented on the effect of countermeasure length, alignment, relative position and material on protection efficiencies. Previous literature, which will be reviewed in Chapter 2 and 3, has revealed the primary parameters of spur dikes are protrusion length, number of spur dikes, distance between spur dikes, and angle to flow. The primary parameters for parallel walls are length, plan shape, and construction material. And the primary parameters for collars that are attached around piers are streamwise length, protrusion width, and vertical position of collar relative to the riverbed. These parameters of different countermeasures will be investigated experimentally under clear-water and live-bed scour conditions.

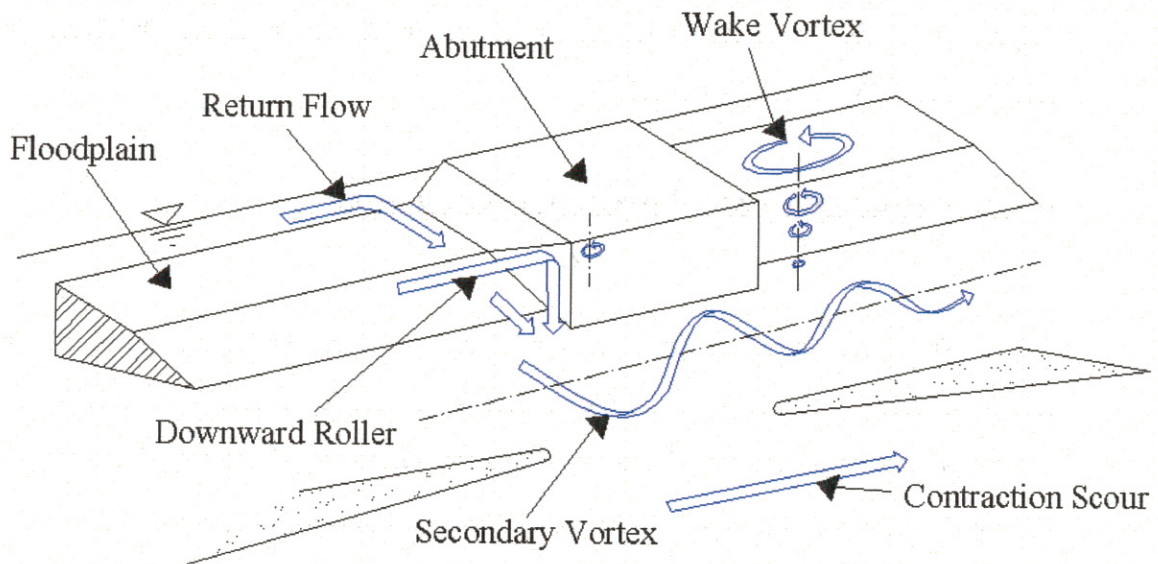


Figure 2-1: Flow patterns around a wing-wall abutment.

Molinas et al. (1998) studied experimentally the shear stress distribution around vertical wall abutments. For Froude numbers ranging from 0.30 to 0.90 and for protrusion ratios of 0.1, 0.2 and 0.3 it was found that the highest values of shear stresses occur at the upstream abutment corner. In the experimental study, shear stresses around vertical wall abutments were amplified up to a factor of 10 depending upon flow conditions and abutment protrusion ratios. It was also found that shear stress amplification due to local effects at the nose region of a vertical wall is a function of the opening ratio and turning angle. Shear stress amplification due to channel restrictions is a function of opening ratio, approach Froude number, and protrusion length. Both formulas for estimating shear stress amplification due to local effects at the nose region of vertical wall abutments and for estimating shear stress amplification due to channel restriction are proposed. The sum of the two shear stress amplifications equals the total nose shear stress amplification.

Ahmed and Rajaratnam (2000) investigated the flow around a 45° wing-wall bridge abutment. It was found that the approach flow turns into a complex 3D skewed flow in the upstream and surrounding regions of the abutment. The bed shear stress was found to increase substantially near the abutment, reaching a peak value of $\tau/\tau_0 \approx 3.63$ at the

It is established that the local scour depth increases progressively with time and reaches equilibrium. Three phases have been identified by various researchers including Gill (1972), Wong (1982), Tey (1984), Kwan (1984), Ettema (1980), Kandasamy (1985) and Dongol (1994) as the initial, the principal, and the equilibrium phases, which can be shown by the different slopes on the plots of the scour depth against the logarithm of time.

A number of approaches concerning the quantitative description of the time evolution of scour depth around abutments, spur dikes and cylindrical piers exist at present. Most of them apply to the principal phase and consist of formulas that include one or more coefficients established experimentally. Among those formulas are Ahmad (1953), Liu (1961), Cunha (1975), Laursen (1963), Ettema (1980), Franzetti et al. (1982), Whitehouse (1997) and Oliveto and Hager (2002). Cunha (1975) concluded that the time to reach the equilibrium scour depth under clear-water conditions is much longer than under live-bed conditions.

2.3.2 The Effect of Flow Velocity

It is well known that when the shear stress the flow exerts on the particles is greater than the critical shear stress that the particles can resist, the particles begin to move and scour starts. For a fully developed turbulent flow like the downflow that causes the scour at the abutment corner and that occurs in natural channels, the total shear stress of the flow can be expressed as (Dongol 1994):

$$\tau = \tau_v + \tau_t = \rho \cdot \iota^2 \cdot (du/dy)^2 = \rho \cdot u_*^2 \quad (2-1)$$

where ι = Prandtl mixing length; ρ = density of water; τ_t = turbulent shear stress; τ_v = viscous shear stress; τ = total shear stress; du/dy = vertical gradient of velocity; u_* = shear velocity.

It can be seen from the equation above that the shear stress of the flow, the shear velocity and the velocity gradient of the flow are related to each other. Generally, the shear velocity ratio u_*/u_{*c} is a good measure of the strength of the downflow and therefore the scouring potential of the vortex structures at abutments. It is often used in the relations of scour prediction equations. But because of the difficulties of measuring the shear velocity under live-bed conditions, the velocity ratio U/U_c has been used in preference to the shear velocity ratio as a measure of the flow intensity.

From data of Dongol (1994) it was found that the scour depth increases almost linearly with flow velocity or shear velocity until the flow velocity reaches the threshold condition. After that, for live-bed conditions, the scour depth varies depending on the bed regime on the approach flow bed. For pier studies with non-rippling sediment ($d_{50} \geq 0.7$ mm), the equilibrium scour depth at first decreases with flow velocity beyond the threshold condition and then reaches a minimum value. Thereafter the scour increases again towards a second maximum with further increase of the flow velocity. Fluctuations of scour depth occur due to an imbalance of the sediment transport into and out of the scour hole. The scour

where U = mean approach flow velocity; U_a = mean approach flow velocity at the armor peak; U_c = mean approach velocity at threshold condition. K_l is formulated to include the sediment gradation effects as well.

2.3.3 The Effect of Flow Depth

Pier scour researchers found that for constant shear velocity ratio, u_* / u_{*c} , the relative scour depth, d_s / D , where D is the diameter of the cylindrical pier, increases at a decreasing rate with increasing normalized flow depth, Y_0 / D , towards a limiting value beyond which the effect of Y_0 / D is negligible. Ettema (1980) showed also that the limiting value of the Y_0 / D ratio for scour depth at piers depends upon sediment size as well. Abutment scour data by Wong (1982), Tey (1984), Kwan (1988), Kandasamy (1989), and Dongol (1994) also showed a similar trend, i.e., the scour depth at abutment increases with flow depth at a decreasing rate towards a limiting value beyond which there is no effect of flow depth. The limiting value of the ratio was found to be about 3 ~ 4. Data from Gill (1972) and Dongol (1994) showed that this limiting value increases as the sediment size decreases. This trend was observed both at clear-water conditions and live-bed scour conditions.

Melville (1992) recommended a flow depth factor K_y to account for the effects of flow depth on scour. This factor will be discussed later with the abutment length factor K_L .

2.3.4 The Effect of Sediment Size

It is important to distinguish between clear-water and live-bed scour when considering the effects of sediment size on scour. Under live-bed conditions, some early pier scour researchers argued that there is no significant effect of sediment size on local scour, but some others suggested that the scour depth decreases with an increase in the sediment size. For clear-water conditions, most studies have shown that sediment size has an effect on local scour.

$$\sigma_g = \sqrt{\frac{d_{84.1}}{d_{15.9}}} = \frac{d_{84.1}}{d_{50}} \quad (2-6)$$

The effect of sediment gradation on scour depth depends upon whether the scour occurs under clear-water or live-bed conditions. For sediment with the same d_{50} and under similar flow conditions, it is found that less scour is developed in nonuniform sediments than in uniform sediments. Scour depth is seen to decrease progressively with increasing σ_g (Ettema (1980), Wong (1982), Melville (1992) and Dongol (1994)).

Data by Ettema (1976) showing the effect of sediment gradation on scour depth at piers at the critical condition are plotted by Dongol (1994) together with data by Wong (1982) for wing-wall abutment. The diagram is plotted using K_σ versus sediment gradation, σ_g , where K_σ is a nonuniform factor defined as:

$$K_\sigma = \left(\frac{d_s}{L(D)} \right)_{\sigma_g} / \left(\frac{d_s}{L(D)} \right)_{\sigma_g=1} \quad (2-7)$$

where $L(D)$ represents the abutment length L if it's abutment and the pier diameter D if it's a pier that is considered.

From that plot it was found that except for rippling sediment, the scour depths for both pier and abutment scour have peak values with $\sigma_g = 1$ and decrease with increasing σ_g . It is attributed to the armoring effects due to the formation of armour layers in the scour holes that protect the underlying finer fractions from erosion and inhibit the scour development. For the rippling sediment at $\sigma_g = 1$, due to formation of ripples and continuous transport of the sediments into the scour hole, a lesser scour depth is observed. At slightly high values of $\sigma_g = 1.5$, a weak armour layer forms stabilizing the bed and inhibiting ripple formation. As a consequence, the scour depth reaches its peak. With even greater values of $\sigma_g > 1.7$, the armoring becomes a prominent feature and a consequent reduction of scour depth is

Kandasamy (1989) studied the scour at abutments under clear-water conditions comprehensively and based on his experimental data he presented a three dimensional graphical relationship to explain the interaction of abutment length, flow depth and scour depth, defining the functional relationship as $d_s = f(L, Y_0)$. He divided the surface defined by the relation $d_s = f(L, Y_0)$ into four different zones.

Zone 1: In this zone, which he called the scour situation as “scour at short abutments”, he found that the scour depth is independent of flow depth. The scour depth increases with the increasing abutment length rapidly and almost linearly. A dead water zone ahead of the abutment is virtually nonexistent.

Zone 2 and 3: In these two zones, according to Kandasamy, scour occurs at medium and intermediate length abutments. The rate of scour depth increase with abutment or flow depth is less than that at a short abutment. A dead water zone develops as a consequence of the greater deflection of flow around the relatively longer abutment.

Zone 4: at very large values of L/y_0 , the ratio reaches the limiting condition and maximum scour depth is observed. The scour situation is termed as “scour at a long abutment”.

Melville (1992) plotted abutment scour data by Gill (1972), Wong (1982), Tey (1984), Kwan (1984, 1988), Kandasamy (1989) and Dongol (1990) as d_s / y versus L / y and d_s / L versus y / L and drew envelope curves to these data. Then he proposed a scour equation as:

$$\begin{aligned}
 d_s &= 10y \quad \text{for } \frac{L}{y} \geq 25 \\
 d_s &= 2L \quad \text{for } \frac{L}{y} \leq 1 \\
 d_s &= 2\sqrt{yL} \quad \text{for } 1 \leq \frac{L}{y} \leq 25
 \end{aligned}
 \tag{2-8}$$

To account for different shapes of abutment, Field (1971), Melville (1992) and some other researchers have proposed different coefficients and relationships for design purposes. The effect of shape is expressed using the shape factor K_s by Melville and the values of the shape factors are given in Table 2-2. The vertical wall abutment is used as a reference. For the spill-through abutment, the abutment length was taken as the length at mid-depth in the water. The shape factors given in Table 2-2 were derived by a procedure to produce the best collapse of data over a range of experimental conditions. These data included Gill (1972), Wong (1982), Tey (1984), Kwan (1984, 1988), Kandasamy (1989) and Dongol (1990) and were all obtained at the threshold condition with uniform sediments.

Table 2-2: Shape factors (Melville 1995)

Abutment shape	Shape factor K_s
Vertical plate or narrow vertical wall	1.0
Vertical wall abutment with semicircular end	0.75
45° wing wall	0.75
Spill-through (H:V):	
0.5:1	0.60
1:1	0.50
1.5:1	0.45

The effects of abutment shape are included by applying the shape factor given in Table 2-2. It is postulated that the importance of abutment shape should diminish as the abutment including the bridge approach embankment becomes longer, because the effect of shape is wrought only at the end of the abutment. An adjusted shape factor was recommended by Melville (1992) for different values of L/y , i.e.,

show that the scour depth decreases with increasing skewness while data by other researchers show contradictory results. Dongol (1994) argued that the short running time of their experiments compared to Kwan and Kandasamy's casts doubt on the equilibrium scour depths. For design purpose, Melville (1992) proposed an abutment alignment factor K_θ and recommended an envelope curve drawn to these data. The effect of abutment alignment depends on the abutment length. It is postulated that the importance of skewness should diminish as the abutment becomes shorter. Melville recommended using an adjusted alignment K_θ^* factor for different limits of L/y , i.e.,

$$\begin{aligned}
 K_\theta^* &= K_\theta \quad \text{for } \frac{L}{y} \geq 3 \\
 K_\theta^* &= K_\theta + (1 - K_\theta) \left(1.5 - 0.5 \frac{L}{y} \right) \quad \text{for } 1 < \frac{L}{y} < 3 \\
 K_\theta^* &= 1 \quad \text{for } \frac{L}{y} \leq 1
 \end{aligned}
 \tag{2-10}$$

2.3.9 The Effect of Approach Channel Geometry

The approach channel geometry can have a very significant influence on the local scour depth at bridge abutments, particularly for long abutments. Bridge abutments can be set back from the natural stream bank or can project out into the flow, and there can be varying amounts of over-bank flow that are intercepted by the approaches to the bridge and returned to the stream at the abutment. The scour at an abutment can be caused by the abutment projecting into the flow, by the bridge approaches intercepting overland flow and forcing it back into the channel at the abutments, or a combination of conditions, as discussed by Richardson et al. (Melville, 1992).

Melville (1995) has classified abutment scour as three basic cases. Case I applies to a bridge spanning a well-defined river channel with no floodplain. In Case II, the bridge approach spans the floodplain and protrudes into the main channel of a compound river channel, the abutment being sited in the main channel. In Case III, the bridge approach and

By assuming equal slope in the main and flood channels the geometry factor K_G simplifies to:

$$K_G = \sqrt{1 - \frac{L_f}{L} \left[1 - \left(\frac{y_f}{y_m} \right)^{5/3} \left(\frac{n}{n_f} \right) \right]} \quad (2-13)$$

By assuming equal roughness in the main and flood channels the geometry factor K_G simplifies to:

$$K_G = \sqrt{1 - \frac{L_f}{L} \left[1 - \left(\frac{y_f}{y_m} \right)^{5/3} \right]} \quad (2-14)$$

It was found that both K_G and the scour depth decrease with both increasing L_f/L and y_m/y_f as expected. At high y_m/y_f values, that is, relative shallow flood channels, K_G tends to be independent of y_m/y_f . It was also found that the equation derived slightly overpredicts the experimental data in general.

By assuming equal slope only, equation (2-12) was plotted by Melville (1995). The resulting plot showed K_G varies as a function of y_m/y_f and L_f/L for $n_m/n_f = 1.0$ and 0.2 . It was shown that the effect of slightly higher roughness in the floodplain compared to that in the main channel is a reduction in K_G and hence in scour depth, especially at small values of y_m/y_f , that is, for computed channels having more uniform depth overall. For large y_m/y_f , $L_f/L \approx 1.0$ and small n_m/n_f , that is, for the case of an abutment sited at about the edge of a relatively shallow and rough floodplain, the scour depth can be as small as 10 percent of that in the corresponding rectangular channel. The K_G values predicted using this equation should be confirmed by experiment.

the observed variation in scour hole depth. Through a least-squares regression analysis, they gave the best-fit linear equation of their data as:

$$\frac{d_s}{y_f} = 7.70 \left[\frac{F_f}{M * F_{fc}} - 0.35 \right] \quad (2-16)$$

They argued that the discharge ratio M reflects the influence of the compound-channel geometry and roughness on the flow field, and ultimately on the scour hole depth. The proposed relationship is limited to the range of values covered by the variables in this study.

Sturm and Sadiq (1996) conducted an experimental study of the depth of clear-water scour around the end of a square-edged bridge abutment terminating in the floodplain of a compound channel. It is indicated that a discharge contraction ratio arising from a theoretical contraction scour analysis for equilibrium conditions can be used for explaining the effect of flow distribution on the local abutment scour depth in the case where significant backwater occurs from bridge contraction. The use of reference values of approach flow depth and velocity in the floodplain for undisturbed conditions without the bridge is shown to collapse experimental results for scour depth in both the case of a contraction with negligible backwater and the case of a contraction with significant backwater in the bridge approach section.

Sturm and Chrisochoides (1997) investigated experimentally clear-water scour around a bridge abutment for variable embankment lengths in a compound channel with the setback of the abutment face relative to the edge of the main channel varying from 0.17 to 0.66 for three different sediment sizes and two different channel cross-sections. They found that both measured and numerically predicted velocities U_a in the local scour region near the face of the upstream end of the abutment at initiation of scour explain, at least in part, the measured values of equilibrium scour depth.

where U_{ab} = the maximum resultant velocity at the upstream corner of the abutment face; y_{ab} = floodplain flow depth at the location of U_{ab} in the contracted section; U_c = critical velocity. In this second formulation, scour depth is related to local values of the hydraulic variables near the face of the abutment. The first formulation requires a one-dimensional numerical flow model to compute the scour prediction variables while the second formulation needs a two-dimensional numerical model to compute the required flow variables. Both formulations are tested with a series of experimental data collected in laboratory compound channels having three different geometries and three different sediment sizes and a similar degree of correlation for each of the formulations is shown by regression analysis.

Cardoso and Bettess (1999) conducted experiments in a compound channel using abutments that extended different distances onto the floodplain including right up to the edge of the main channel (Melville, Type III) to study the effect of time and channel geometry on scour at those abutments. The experiments were performed with flow on the floodplain being critical. They found that for clear-water scour the equilibrium was reached after 68 hours on average, and for live-bed conditions equilibrium was attained after 10 hours on average. The three phases were identified in the time development of the scour. Moreover, the scour development in the principal phase is well described by the theories of Ettema (1980), Franzetti (1982), and Whitehouse (1997). However, time needed for clear-water scour to reach the equilibrium state seems to vary with sediment size. Sturm and Janjua (1993) found that for sediment size of 3.3 mm it only took 12~16 hours to reach a state when there was no further movement of sediment out of the scour hole, which implies the equilibrium state is reached.

Cardoso and Bettess (1999) found in their experiments that unless the abutment approached to the edge of the main channel, there was little interaction between the flow in the main channel and flow on the floodplain. They also found that as the ratio of the abutment length to the floodplain width L/L_f tends from smaller than 1 to 1, increase of scour depth was not found at the tip of the abutment; on the contrary, their data indicate a flattening

CHAPTER 3. A LITERATURE REVIEW ON BRIDGE ABUTMENT SCOUR COUNTERMEASURES

3.1 Introduction

A wide variety of countermeasures have been used to control channel instability and scour at bridge foundations. In HEC-23 (Lagasse et al., 1997) a countermeasure matrix is organized to highlight the various groups of countermeasures and to identify their individual characteristics. Countermeasures have been organized into groups based on their functionality with respect to scour and stream instability. The three main groups of countermeasures are: hydraulic countermeasures, structural countermeasures, and monitoring. Hydraulic countermeasures can be further classified as river training structures and armoring countermeasures.

Countermeasures for local scour at abutments consist of countermeasures that improve flow orientation at the bridge end and move local scour away from the abutment, as well as revetments and riprap placed on spill slopes to resist erosion.

Selected countermeasures including spur dikes, guide banks and collars will be reviewed and studied subsequently.

3.2 Spurs dikes

3.2.1 Introduction

Spur dikes have been studied intensively for many years mostly as river training or river rehabilitation structures instead of abutment scour countermeasures. Studies on spur dikes include Lacey (1936), Inglis (1949), Mushtaq Ahmad (1953), Laursen (1953, 1962b), Andru and Blench (1957), Iwagaki (1958), Garde (1961), Liu et al. (1961), Cunha (1973), Gill (1972), Garde (1961), Franco (1982), Copeland (1983), Rajaratnam and Nwachukwu (1983a), Zaghoul (1983), Brown (1985), Suzuki et al. (1987), Khan and Chaudry (1992), Wu and Lim (1993), Molis et al. (1995), Mayerle et al. (1995), Muneta and Shimizu (1994), Tominaga et al. (1997), Zhang and Du (1997), Soliman et al. (1997), Farsirotou et al. (1995),

experience and practices within specific geographical areas. This is due to the wide range of variables affecting the performance of the spur dikes and the differing importance of these variables with specific applications. The main site-specific parameters affecting the performance of the spur dikes include: channel width, depth, flow velocity, shape of flow hydrographs, sinuosity of the channel, bed material size distribution and transport rate, material characteristics of the bank (Copeland, 1983). Parameters that affect the performance of spur dikes include length, width, height, shape, orientation angle, permeability, construction materials, and longitudinal extent of the spur dike field (Melville and Coleman, 2000).

Spur dikes may be classified based on their permeability: high permeability - retarder spur dikes; impermeable - deflector spur dykes; and intermediate permeability - as retarder/deflector (Brown, 1985). Permeability of a spur dike may be defined as the percentage of the spur dike surface facing the flow that is open. A permeable spur dike of the hurdle or pile cluster type has the advantage of slowing down the current instead of deflecting it, thus hastening the deposition of sediment and building up of the high ground and the bank lines. This is especially effective on rivers carrying a considerable amount of suspended sediment. Permeable spur dikes have been used in India and Pakistan as a temporary measure to meet exigencies with success. But permeable spur dikes have their draw-backs. Because (1) they are not as strong as the solid types in resisting the forces exerted by floating debris or ice; (2) they are a nuisance to navigation during high water period if built low, and the cost of long piles may be prohibitive if built high; (3) the best type of permeable construction is obtained by using piles, but this would not be feasible where the river bed is of gravel and boulders; they will not resist the flow very well unless they be of the tetrahedral type such as those used in California and Japan, where slant posts connected to base beams are weighted down by concrete blocks or stones in wire crates (The United Nations 1953).

A qualitative guide as to the type of spur dike to use for a specific situation is given in a table in Lagasse et al.(2001). This table provides preliminary advice on the type of spur dike that may be most suitable for a given circumstance.

ranging in size from 0.06 mm to 0.37 mm, Inglis concluded that gradation is a factor affecting the maximum scour. His study also indicated that the maximum scour depth depends on local discharge (on the local mean velocity of flow).

Ahmad (1953) conducted investigations on the behavior of spur dikes using sand of 0.37 mm and 0.7 mm mean diameter and drew some valuable conclusions regarding the effect of various parameters on the maximum scour. He studied the effect of different discharge intensity, sand grade, flow concentration and angle of the spur dike to flow on the scour depth and scour pattern around a spur dike. He gave a formula for calculating the scour depth at a spur dike nose for different conditions of flow concentration and angles of approach based on the experiments. He also determined the shape of the falling apron in plans for different types of spur dikes and for various angles of approach to a T-headed spur. He was of the opinion that the maximum scour depth is unaffected by change in the sediment grade. But the rate of the development of the scour is much more rapid with finer sand.

Laursen (1953) has stated that scour around bridge piers is a function of depth of flow and is independent of mean velocity and size of bed material for a given opening ratio. Laursen (1962b) maintained that under conditions of no sediment supply, such as a relief bridge, the velocity and the sediment size are important in determining the depth of scour and that under conditions of sediment supply by the approach flow well above the critical tractive force, the velocity and sediment size have little effect except insofar as they determine the mode of sediment movement.

Andru and Blench (1957), after analyzing various laboratory and field data on the scour at obstructions, concluded that the depth of local scour depends on discharge intensity and the size of bed material. Izzard and Bradley (1957) feel that the sediment size and gradation affects only the rate of development of scour hole and not the maximum scour hole.

Also according to Iwagaki (1958), the size of the material is important in the study of scour, and the drag coefficient C_D is a significant parameter that takes into consideration the size and the specific weight of the sediment.

material and the flow depth was empirically formulated.

Copeland (1983) carried out model tests in a 130- by 50ft sand bed flume with a channel top width of 8ft and an average depth of 0.24ft. The stream sinuosity was 1.6 and the slope was 0.0012. He suggested that the coarse fraction of the bed material is an important factor that affects the scour depth around the spur dike.

Rajaratnam and Nwachukwu (1983a) tried to study the flow structures near spur dikes by measuring the flow in a straight tilting rectangular flume, 120 ft long, 3 ft wide and 2.5 ft deep with smooth bed and sides. Most of the tests were done with a smooth bed. They found that when a groin is placed in a channel, it causes a significant disturbance to the flow for a short distance upstream and for a longer distance downstream. The disturbed flow was analyzed by splitting it into a deflected flow region and a shear layer. For the deflected flow region, the skewed turbulent boundary layer model of Johnston was found to be valid. In the shear layer, the velocity distributions for any horizontal plane were found to be similar. They also found that the maximum bed shear stress occurred near the groin nose. The shear stress amplification τ/τ_o varies with the ratio of the length of groin and the width of channel b/B . The τ/τ_o ratio was 5 and 3 for the 6-in. and 3-in. groin respectively.

Zaghloul (1983) conducted experiments in a 36 ft long, 1.5 ft wide and 2 ft deep aluminum flume with Plexiglas wall to study the effects of upstream flow conditions, sediment characteristics, and spur dikes' geometry on the maximum scour depth and scour pattern around a spur dike. Through dimensional analysis and experimental data verification, he found that the maximum scour depth is significantly affected by the opening ratio of the channel and the Froude number of the flow. He also came up with a maximum scour depth prediction equation which he found is identical in form to the regime equations by Lacey and Blench. His experiments were conducted under clear-water conditions but most runs were run for only 2.5 hours.

Suzuki et al. (1987) performed experiments to discuss the characteristics of the local bed form around a series of spur dikes in an alluvial bed with continuous sediment motion.

Kuhnle et al. (1997, 1998, and 1999) performed a series of experiments in a flume with 30 m length, 1.2 m width, and 0.6 m height to investigate the volume of scour holes associated with spur dikes. By varying the spur dike orientation angles, overtopping flow height, and the contraction ratio, respectively, they found that: (1) the contraction ratio and flow depth are positively correlated with the volume of the scour for a given elapsed time under steady flow; (2) the geometry of the scour hole has been shown to be affected by the value of the overtopping ratio. The larger the overtopping ratio is, the greater is the erosion of the bed in the near bank region and the more the region of maximum scour shifts toward the channel bank. It also caused a secondary scour zone to form downstream of the spur dike; (3) for the three angles of spur dike and two contraction ratios being considered, 135° spur dikes had the lowest, 90° spur dikes had an intermediate value, and 45° had the highest bed erosion in the vicinity of the channel bank. The volume of the scour hole was greatest for the 135° spur dikes. They also presented a simple procedure to predict the area and volume of scour around spur dikes.

In addition, a series of studies of the local scour phenomenon around bridge abutments were also carried out by various investigators. These studies have been reviewed in a previous chapter.

3.2.3 Empirical Formulas

Some equations for predicting the scour depth at the nose of spur dikes are listed below and all of them are empirical equations. These equations were derived from tests in laboratory flumes with limited verification by prototype testing. There has been a general lack of agreement of the important variables needed to predict maximum scour depth. This disagreement has been possibly settled by Melville (1992, 1997) in which the ratio of the length of the structure to the flow depth determines the form of the equation. Melville's (1992) equations were technically derived for bridge abutments, however, in many cases, particularly in experimental studies, model bridge abutments are similar to spur dikes since they are structures with similar characteristics.

$$y_s = 2K_s^* K_\theta^* (yL)^{0.5} + y \quad 1 < \frac{L}{y} < 25$$

$$\frac{y_s}{y} = 3.36 F_n^{0.488} (U/U_c)^{0.788} (L/y)^{0.538} (B_1/y)^{-0.142} \quad \text{Zhang and Du (1997)} \quad (3-13)$$

where B_1 = original channel width, B_2 = constricted channel width, C_D = drag coefficient, D_{50} = median grain size, σ_g = geometric standard deviation of the bed material, F_{bo} = Blench's zero bed factor which is a function of grain size, F_n = Froude number, f = Lacey silt factor, g = acceleration of gravity, k = function of approach conditions, K = function of C_D which varies between 2.5 and 5.0, L = effective length of spur dike, $L' = A_e / y$, A_e = flow area of an approach cross section obstructed by a roadway embankment, n = function of C_D which varies between 0.65 and 0.90, Q = total stream discharge, q_2 = discharge per unit width at constricted section, r = assumed multiple of scour at spur dike taken as 11.5 by Laursen, U = average velocity in unconstricted section, y = average depth in unconstricted section, y_s = equilibrium scour depth below water surface, ρ = mass density of water, K_s = abutment shape factor by Melville, K_θ = abutment alignment factor by Melville, K_θ^* = adjusted abutment alignment factor by Melville, K_s^* = adjusted abutment shape factor by Melville.

In Equation (3-2), k varies between 0.8 and 1.8. This equation is for spurs projecting straight or upstream with sloping head.

Equation (3-3) is derived from dimensional analysis based on a hypothetical experiment. Because the terminal velocity of sediment is taken as a factor, the equation should be for flow with sediment transport. The coefficient k is determined by experiments and for different positions and flow conditions. It has different values ranging from 1.2 to 2.25.

The author of Equation (3-4) first carried out dimensional analysis and concluded that the maximum scour depth is a function of opening ratio, spur inclination angle to the channel, Froude number of the flow, and the drag coefficient of the sediment. Then he plotted his data

In Equation (3-10), K is a coefficient depending on the lateral scour hole slope. K=0.68, 1.1 and 1.36 for lateral slopes 10°, 25° and 35°, respectively.

Equation (3-11) is for clear-water scour. For live-bed scour condition, the regression model reduces to

$$\frac{y_s - y}{y} = 2.27 K_s K_\theta \left(\frac{L}{y}\right)^{0.43} F_a^{0.61} \quad \text{Froehlich (1989)} \quad (3-14)$$

$K_s=1.0$ for a vertical wall abutment that has square or rounded corners, and a vertical embankment; 0.82 for a vertical abutment that has wingwalls and a sloped approach embankment; and 0.55 for a spillthrough abutment and a sloped approach embankment. $K_\theta = (\theta/90)^{0.13}$. For design purpose, the author recommended that a factor of safety be added to the value of maximum relative depth of scour computed using Eq. (3-11) or Eq. (3-14).

Through the analysis of local scour, Melville (1992) established the relationship between d_s / L (or d_s / y) and the multiplication of a series of K factors. The K factors are expressions describing the influence of each parameter including flow intensity, flow depth, sediment size, sediment gradation, abutment length, abutment shape and alignment and approach channel geometry. Using laboratory data available, the author tried to determine each of these K values and finally obtained Equation (3-12). Because of a lack of data, these three equations do not include the effects of sediment characteristics, lateral distribution of flow, or river geometric features including over bank flow and may lead to conservative estimates of scour depth in some instances. However, the design method has the advantage of simplicity.

Zhang and Du (1997) did experiments in a flume of 2.4 m wide and 26 m long to study the maximum scour depth around spur dike using sand bed of average sand diameter of 0.66 mm. The median size of the sand is 0.60 mm and the standard deviation of the sand size distribution is 1.90. For spur dikes perpendicular to the flow and maximum scour condition, they proposed Equation (3-13) using dimensional analysis and regression analysis techniques

\bar{d}_s - Dimensionless maximum scour depth, ϕ = rest angle, \bar{b} = dimensionless abutment length, β = constant for flow concentration.

The model above was compared with previously-proposed formulae by Laursen (1962), Melville (1992), and Lim (1997) for the prediction of maximum scour depth ($u_* = u_{*c}$). The prediction by the present model was found to be situated in the middle of the previous formulae. But the present model is not able to explain the experimental features of long abutments ($L/y > 25$) where d_s/y takes a constant value (=10) according to Melville's empirical formula. Moreover, the effect of Fr on d_s/y in supercritical flows is uncertain.

3.2.5 Numerical Simulations around Spur Dikes

The most important aspects to be considered in the spur dike design are the layout, plan view, shape, length, spacing, crest longitudinal shape, crest elevation, orientation, permeability, construction materials and local scour (Alvarez, 1989). The majority of these aspects can nowadays be examined with numerical models. Numerical model simulations are usually more cost-effective and faster than physical model studies, and have no inherent limitation on spatial extent.

Zaghloul et al. (1973) solved the Helmholtz vorticity equation and Poisson type equation using constant eddy viscosity. The velocity and vorticity distributions were obtained but computed velocities were not compared with any experimental results.

Tingsanchali (1990) used a two-dimensional depth-averaged equation and a $\kappa - \varepsilon$ model to close the Reynolds' stresses. The velocities agreed with the experimental data when a correction factor for the streamline curvature was applied to the $\kappa - \varepsilon$ model.

Khan et al. (1992) tried to simulate the flow around spur-dikes by solving the depth-averaged Navier-Stokes equations using a two-dimensional mathematical model. MacCormack's explicit finite difference scheme was used and the equations were solved first by neglecting the effective stresses and then by including the turbulent stresses. In all his

and gave reasonable flow patterns. However, it should not be applied indiscriminately since the mixing length is based on measurements in straight rectangular channels.

Molls et al. (1995) numerically simulated the flow near a spur-dike by solving the depth-averaged equations using both an implicit ADI scheme and the explicit MacCormack scheme. Both inviscid and viscous solutions were obtained. A constant eddy viscosity model was used to close the effective stresses with the viscosity near the spur obtained from the dimensionless, turbulent, eddy viscosity reported by Tingsanchali and Maheswaran. Also an assumption of constant eddy viscosity near the spur throughout the entire flow field was made. The ADI scheme was solved in conjunction with a packed grid and the velocity field and recirculation length closely matched the experimental data and computed results obtained by Nawachukwu and Tingsanchali and Maheswaran, respectively. It was demonstrated that, provided with a reasonable estimate of the eddy viscosity near the spur, the constant eddy viscosity model produces results similar to those obtained with more advanced turbulence models. Through a sensitivity analysis, the ADI scheme was found to be insensitive to Chezy C but very sensitive to turbulent viscosity.

Interestingly, Molls' ADI scheme, Tingsanchali and Maheswaran's (1990) TEACH model and the MacCormack scheme underpredict the experimental velocities at a certain location downstream of the spur.

Soliman et al. (1997) used a 2-D mathematical model (TRUSOLA) to simulate a Nile bend located about 3 km downstream of Naga Hammadi barrage. In this model, the shallow water assumption is used to model the flow, and the vertical momentum equation is reduced to a hydrostatic pressure relation. The vertical water motion is derived from the horizontal flow field using the continuity equation. The program followed the Boussinesq approximation. Different lengths and spacing were used to simulate the effect of spur dikes on water levels and velocity components. About fifty runs were carried out. The author concluded that: (1) spur dikes would cause appreciable increase in the head upstream if it constricted more than 6% of the channel width; (2) A pocket of deposited material occurs between the spurs for all tests with spacing less than $4L$ but disappeared for a spacing of $7L$.

location of spurs (whether on concave banks or convex banks), and the cost of construction etc. So the spacing of spurs could be varied according to different design conditions. A spacing of 2 to 2.5 times of the length of spurs is the general practice. For the length of spurs, no general rules can evidently be formulated. It depends entirely on the exigencies arising in a specific case. But length should not be shorter than that required to keep the scour hole formed at the nose away from the bank. Normally spurs longer than 1/5 the river width are not provided.

Alvarez (1989) recommended that the length of the spur dikes should be kept between the following limits $y \leq L \leq 0.25B_1$ when the river bank is almost parallel to the river axis, where y and B_1 are the mean flow depth and the mean width of the free flow surface. Also when spur dikes are built in straight stretches without anchoring in the bank, the spacing should be 4L to 6L, where L is the working spur dike length. If the curve is regular with only one curvature radius, 2.5~4L is optimum; if the curve is irregular, the spacing should be found graphically. Recommendations from several sources are shown in Table 3-1.

3.2.6.2 Orientation of Spur Dikes

The orientation of spur dikes has typically been determined by experience in specific geographical areas and by preference of engineers. There is considerable controversy as to whether spur dikes should be oriented with their axis in an upstream or downstream direction.

Thomas and Watt (1913) concluded that the various alignments were probably of slight importance. Franzius (1927) reported that spur dikes directed upstream are superior to normal and downstream-oriented spur dikes with respect to bank protection as well as sedimentation between the dikes.

Strom (1941) reported that the usual practice in New Zealand was to incline impermeable groins slightly upstream, but that downstream-oriented spur dikes had also been used successfully. Strom stated that a spur dike angled downstream tends to swing the current

angle varying between 100 and 120 degrees was recommended for bank protection. It also discussed how to build a system of spur dikes.

Mamak (1964) stated that dikes are usually set perpendicular to the flow or set upstream at angles between 100 and 110 degrees.

Lindner (1969), reporting on the state of knowledge for the U. S. Army Corps of Engineers, stated that there has not been a sufficiently comprehensive series of tests either in the field or by model to conclude that any acute or obtuse angle for the alignment at dikes is superior or even as good as perpendicular to flow. Thus, he recommended perpendicular dikes except in concave bendways where they should be angled sharply downstream. Neill (1973) recommended using upstream-oriented dikes. After reviewing much of the literature on spur dikes Richardson and Simons (1973) recommended perpendicular spur dikes, suggesting that spur dikes with angles between 100 and 110 degrees could be used to channelize or to guide flow.

In the United States, the U. S. Army Corps of Engineers (1978) has generally oriented its spur dikes perpendicular or slightly downstream. On the Missouri River, dikes are generally oriented downstream with an angle of 75 degrees. On the Red and Arkansas Rivers, dikes are placed normal to flow or at angles of 75 degree. The St. Louis District uses both perpendicular and downstream oriented dikes. The Los Angeles District (1980) used dikes with an angle of 75 degrees pointing downstream.

As late as 1979, Jansen (1979) concluded that there is no definite answer as to whether spur dikes should be oriented upstream or downstream, and recommended using the cheapest solution---that being the shortest connection between the end of the dike and the bank. This corresponds with Lindner (1969). Copeland (1983) found that the scour depth was more severe for spur dikes with an upstream orientation than for those with a downstream orientation. And he found there is no indication that the scour hole is closer to the bank for spur dikes pointed downstream. He concluded that the spur dike should be oriented perpendicular to the bank to obtain the most effective bank protection.

3.2.6.3 Permeability

Permeability of spur dikes is a very important factor that affects the function of the spur dikes and also an important design consideration. Generally, it is believed that the greater the spur dike permeability, the less severe the scour pattern downstream of the spur tip, the lower the magnitude of flow concentration at the spur tip. The more permeable the spur, the shorter the length of channel bank protected downstream of the spur's riverward tip.

Brown (1985) gave some recommendations for application of different spur permeability for different purposes as follows: (1) where it is necessary to provide a significant reduction in flow velocity, a high level of flow control, or where the structure is being used on a sharp bend, the spur's permeability should not exceed 35 percent; (2) where it is necessary to provide a moderate reduction in flow velocity, a moderate level of flow control, or where the structure is being used on a mild to moderate channel bend, spurs with permeability up to 50 percent can be used; (3) spur permeability up to 80 percent can be used in some special cases but is not recommended; (4) jack and tetrahedron retardance spurs may be used only when it can be reasonably assumed that the structures will trap a sufficient volume of floating debris to produce an effective permeability of 60 percent or less; (5) Henson-type spurs should be designed to have an effective permeability of 50 percent. (6) if minimizing the magnitude of flow deflection and flow concentration at the spur tip is important to a particular spur design, a spur with a permeability greater than 35 percent should be used; (7) impermeable spurs should not be used along channel banks composed of highly erodible material unless measures are taken to protect the channel banks in this area.

Central Board of Irrigation and Power (1989) discussed the construction, types, and application of permeable and impermeable spurs. It stated that permeable spurs have the important advantage of being cheap and are effective only in rivers which carry heavy suspended load. But they are usually not strong enough to resist shocks and pressures from debris, floating ice and logs. Submerged permeable spurs are preferable to submerged solid spurs since the former do not create turbulent and eddy conditions as strong as with the latter in the case of deep and narrow rivers where depths are considerable. Impermeable spurs are

channel flow and inducing more sediment deposition in the dike field than systems with all dikes level and that level dike fields are more effective than stepped-up fields. He also recommended that level-crested dikes be placed normal to the flow or oriented downstream and sloping crested dikes be normal to the flow or oriented upstream.

There are different spur head forms that function quite differently when placed in the river channel. Ahmad (1953) classified them in four types as straight, hockey, inverted hockey and T-headed. His tests showed that the maximum depth of scour and area of the apron needed at the T-headed spur are relatively small compared with straight and hockey spurs. He also concluded that the T-headed spur is economical in stone. The interesting thing to be noticed from his data is that the minimum scour depth occurred at the inverted hockey spur.

Franco (1967) performed experiments with the length of the L-head (similar to inverted hockey type spur by Ahmad) equal to half of the distance between the ends of adjacent dikes. He found that the L-head tended to prevent sediment-carrying bottom currents from moving into the areas between the dikes. Maximum scour depth at the ends of the dikes was reduced appreciably, as was the elevation of deposition between spur dikes.

In a series of tests by Linder et al. (1964) it was found that the L-head should close 45 to 65 percent of the gap between the dikes in a dike field, and that little benefit was derived from building the L-head above the water surface. The results indicated that the L-heads decreased the scour around the ends of the spur dikes compared with stubbed-off dikes, and improve navigation conditions and depths by reducing eddy disturbances and by causing the contraction to persist more continuously along the dike system, thus producing more uniform bed configuration and consistent depths. In addition, almost any reasonable degree of closure will give added protection to the concave bank over no closure at all. However, L-heads are expensive so that additional testing and experience are needed to show whether their merits are sufficient to recommend their general use in connection with channel contraction.

J-heads, which are similar to hockey-stick-shaped spur dikes, together with T-heads

3.2.7 Application of Spur dikes

Spur dikes are used to alter flow direction, induce deposition, or reduce flow velocity. Their main use is to protect banks that contain bridge abutments from eroding. Spur dikes are commonly used to realign streams as they approach a bridge abutment. A bridge abutment may be in danger of being severely eroded when it is subjected to high velocity flow from a channel that has changed course due to meandering of the channel. Spur dikes may also be used to establish and maintain the alignment of a channel. They have been used to decrease the length of the bridge required and reduce the cost and maintenance of the bridge in actively migrating braided channels (Lagasse et al., 2001).

A groin with a submerged dike at its toe was constructed on the coast of Washington to protect a stretch of state highway from destruction due to shore erosion. It was found that the structure performed well as expected and has helped relocate the deep tidal channel 500 to 2000 feet further away from the shore in spite of some expected scour development at the toe of the dike (Sultan et al. 2002).

According to Richardson et al. (1984), spurs may protect stream banks at less cost than riprap revetment, and by deflecting the current away from the bank and causing deposition, they may more effectively protect banks from erosion than revetment. Uses other than bank protection include the constriction of long reaches of wide, braided streams to establish a stable channel, constriction of short reaches to establish a desired flow path and to increase sediment transport capacity, and control of flow at a bend.

3.3 Hardpoints

Hardpoints consist of stone fills spaced along an eroding bank line, protruding only short distances into the channel. A root section extends landward to preclude flanking. Hardpoints are most effective along straight or relatively flat convex banks where the streamlines are parallel to the bank lines and velocities are not greater than 3 m/s within 15 m

Guide banks can protect not only bridge abutments from local scour, but also the approach embankment because of the still water area behind it. When embankments span wide floodplains, the flows from high waters must be aligned to flow smoothly through the bridge opening. Overbank flows on the floodplain can severely erode the approach embankment and could increase the depth of the scour at the bridge abutment. Guide banks can be used to redirect the flow from the embankment and to transfer the scour away from the abutment. Guide banks serve to reduce the separation of flow at the upstream abutment face and maximize the total bridge waterway area, and reduce the abutment scour by lessening the turbulence at the abutment face (Lagasse et al., 2001).

There are practically two kinds of guide banks. One is the American practice, which is to give guide banks an elliptical form convergent to the opening, whereas the other in Pakistan and India, guide banks are straight and parallel to the opening with a curved section at the upstream and downstream ends. Mahmood stated that parallel guide banks straighten the flow more effectively than convergent ones (Richardson et al., 1984).

Design guidelines for guide banks are given in Neil (1973), Bradley (1978), Ministry of Works and Development (1979), Central Board of Irrigation and Power (1989) and Lagasse et al. (1995).

3.4.2 Experimental Studies

Karaki (1959, 1961) carried out a laboratory study in a flume 16 ft wide and 84 ft long with an erodible bed for clear-water flow on the floodplain with a spill-through abutment, wing-wall abutment and skewed embankments models. He concluded: (1) guide banks are effective measures to reduce scour at bridge abutments and the effectiveness of guide banks is a function of the geometry of the roadway embankments, flow on the floodplain, and size of bridge opening. (2) The proper location for an earth embankment guide bank is at the abutment with the slope of the guide bank tangent to the slope of the abutment. (3) Curved guide banks are more efficient than straight ones because of the smoother streamlining of the flow. He graphically set forth tentative criteria for design

desirable feature of this design was that the train of secondary scour holes passed through the position of the first piers and caused an increase in pier scour. The 30-cm guide wall also produced ideal protection for the abutment and no increase in pier scour, but head end scour was increased about 1 cm to 4.8 cm. With the half-cell on the upstream face of the abutment, a conical scour hole of 6.0 cm deep developed. The scour extended so far around the half-cell that the approach grade was severely scoured on one side and the footing was exposed on the other. It was concluded that the half-cell was not a satisfactory alternative. The 30-cm wall was considered to be the most promising. However, a single wall cantilevered out of the river bed was considered vulnerable to damage by ice and also of questionable stability if there was scour on the flow side and no scour on the other side. Accordingly, a variation of a 30-cm wall was selected for further study, and consisted of a multi-cell guide wall of the type so often used for steel cofferdams. It was found that this wall not only can protect the abutment as well as the former 30-cm wall, but also shows more stability than the first one. It was concluded that abutment scour could be controlled with an earth guide bank, consisting of a 30-cm cellular sheet pile guide wall. Test results for the cellular steel guide wall were judged to be most reliable in terms of predicting prototype behavior, and this design appeared to give an ideal solution. A particularly desirable feature of the guide wall was that it eliminated all attack on the upstream face of the highway grade at the abutment. In 1970 it was decided to add an earth guide bank to the existing riprap protection. The most recent sounding in June 1981 showed no change in riprap position, and the abutment was well protected by the combination of the guide bank and the riprap.

3.4.3 Guide Bank Design Considerations

The important factors for guide bank design are orientation relative to the bridge opening, plan shape, length (upstream and downstream of the abutment), cross-sectional shape, crest elevation, and protection of the structure from scour. These aspects are discussed below.

increase of the width of spread of the concentrated flow, which leads to a reduction of local velocity and results in smaller depth of scour. However, Herbich (1967) suggested that length of guide banks are not important provided they are over a certain length and this is usually satisfied when a certain shape is developed.

Spring (1903) has the opinion that the length of guide bank is dependant on the following considerations: first, the distance necessary to secure a straight run for the river through the bridge; and secondly, the length necessary to prevent the formation of a bend of the river, above and behind the guide banks, circuitous enough to breach the main railway approach bank; thirdly, it depends to a certain extent on the length of the bridge for a given river, provided that the bridge is designed so that all its spans shall be acting fairly equally, instead of some having considerably more flow than others; fourthly, the upstream length of the guide banks is dependant also to some extent on the breadth of the unnarrowed river.

Spring suggested that (1) the length of the upstream part of the guide banks may be made equal to or up to a tenth longer than the bridge. But close attention should be paid to the possibility of the river eroding the main approach bank. In especially wide rivers this may involve the use of very long guide banks; (2) the length of the downstream part of the guide bank may be a tenth to a fifth of the length of the bridge so that the swirl downstream of the bridge can be kept far enough away not to endanger the approach bank.

Karaki (1959, 1961) gave a tentative method to determine the length of the guide banks based on the laboratory data obtained. Based on the information obtained from model studies performed at Colorado State University, field data collected by the U.S. Geological Survey during floods in the State of Mississippi, and field observations by Schneible during floods, Bradley (1978) developed a chart for determine the length of guide banks. In this chart, the discharge ratio Q_f / Q_{100} (Q_f is the lateral or floodplain flow on one side measured at a certain section, cfs; Q_{100} is the discharge in 100 feet of stream adjacent to abutment, measured at a designated section, cfs.) is shown as the ordinate, the length of dike L as the abscissa, and the family of curves are for different values of the average velocity through bridge opening. He also suggested that for skewed crossings, the length of guide banks be set

guide banks is that the cost of an unduly long bridge may be saved. Therefore, instead of building a high wall on deep foundations, the engineer makes his guide banks of sand and earth on a plan suitable for the proper guidance of the river currents and for the discouragement of swirls; then he lays such a covering of loose stone, boulders, riprap, or one-man-rock, over the exposed part of them, as will serve to protect them against every conceivable kind of attack to which they are liable (Spring, 1903). Spring stated that in India one-man-rocks weighing from 60 to 120 lbs with irregular angles are suitable for the armoring of the guide bank slopes. Although rocks with high specific gravity, say 3.0, are preferred, rocks with a specific gravity of 2.44 are usually used because of its cheapness and availability. Recommendations for the thickness of stone pitching and soling for permanent slopes required at the head, body, and tail of guide banks, for river flowing in alluvial plains can be found in Central Board of Irrigation and Power (1989).

In the Guidelines for Design and Construction of River Training and Control Works for Road Bridges published by the Indian Roads Congress (1985), the size of stone required on the sloping face of the guide banks on the river side is given as $D_r = 0.0282U^2$ for 2:1 side slope and $D_r = 0.0216U^2$ for 3:1 side slope.

Bradley (1978) suggested that if rock is used as a facing on a guide bank, it should be well graded and a filter blanket should be used if the relative gradations of the rock and of the guide bank material require it. If it is constructed of earth, it should be compacted to the same standards as the roadway embankment and should extend above expected high water.

Riprap can be used to inhibit erosion of the embankment materials. As an alternative, guide banks can be constructed entirely of riprap-size material, if such material is readily available. Rock riprap should be placed on the stream-side face as well as around the end of the guide bank. It is not necessary to riprap the side of the guide bank adjacent to the highway approach embankment. The designer is referred to standard references such as HEC-11 (FHWA, 1989), Richardson et al. (1990), or Pagan-Ortiz (1991) for design procedures for sizing riprap at abutments. Riprap should be extended below the bed elevation to a depth as recommended in HEC-11. Additional riprap should be placed around the

scour depth below the bed level at which the apron is laid. Spring suggested from his considerable experience that it should not be less than 1.5 times the scour depth for the shank and 2 times for the head, as has been adopted also by Gales. In addition to 1.5 times the scour depth, Gales provides an extra 4.6 to 7.6 m width of apron at the foot of the slope, which he calls the berm.

Regarding the thickness of apron as laid, people found that according to Spring's recommendations, when the apron is completely launched, its thickness is less than that of the permanent slope near its toe. This deficiency in the distribution of stone was overcome differently by different engineers. Gales advocated the uniform apron and provision of a berm, which is only an addition length of the apron.

3.4.3.6 Construction and Maintenance

The construction process is important to help keep the cost of guide bank low and guarantee the completion of the guide bank in time. Several factors to be considered are the magnitude of construction arrangements for earthwork, the magnitude of construction arrangements for stone, time available for construction and labor availability.

No matter how well they are designed at the beginning, guide banks may find themselves exposed during some period of their existence, at some part of their perimeter, to scour so severe that there seems danger. Therefore, maintenance work is necessary. Service tracks should be made and maintained in case train loads of stones are required to be transported to a threatened place.

Because stone has to be thrown in from time to time as apron stone gets washed away, maintenance may be very expensive-as exemplified by the case of the Hardinge Bridge, where nearly a million pounds was spent on repairs in a period of two years (Inglis, 1949).

Bradley (1978) suggested that: (1) deep trees as close to the toe of the guide bank

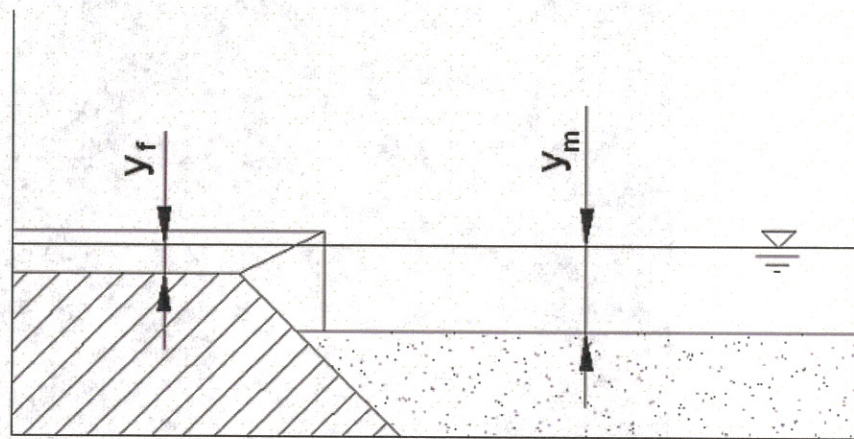
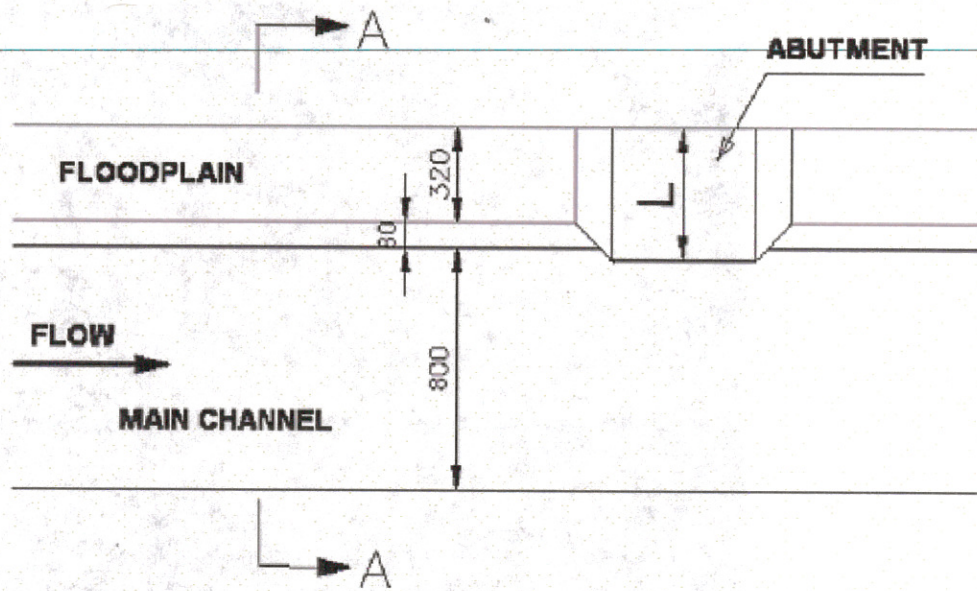
attached around the pier sitting horizontally a short distance from the bed. Papers of collars on abutment scour protection were not found in the literature.

3.6 Summary

Although many studies have been carried out for each of these countermeasures, there are still needs for further studies of their use in protecting bridge abutments. For instance, spur dikes have not specifically been tested and used for abutment protection. Guide banks have been tested and used for spill-through abutments on rivers with wide floodplains or rectangular channel only. For small country bridges with wing-wall abutments terminating on the main channel bank, studies are still needed. In addition, there are many controversial design guidelines and small design issues that need to be clarified. Collars have been tested for pier scour protection rather for abutment protection.

Countermeasures are often damaged or destroyed by the stream, and stream banks and beds often erode at locations where no countermeasure was installed. However, as long as the primary objectives are achieved in the short-term as a result of countermeasure installation, the countermeasure installation can be deemed a success (HEC-23). Therefore, to achieve long-term protection, maintenance, reconstruction, and installation of additional countermeasures as the responses of streams and rivers to natural and man-induced changes is needed.

Among armoring countermeasures, riprap and cable tied blocks are of the most interest by hydraulic engineers. These two countermeasures have been investigated by various researchers as erosion control devices and bank revetments. Since studies of riprap and cable tied blocks are not included here, the literature is not reviewed herein.



SECTION A-A

Figure 4-1: Dimension Sketch for Experimental Compound Channel (mm)

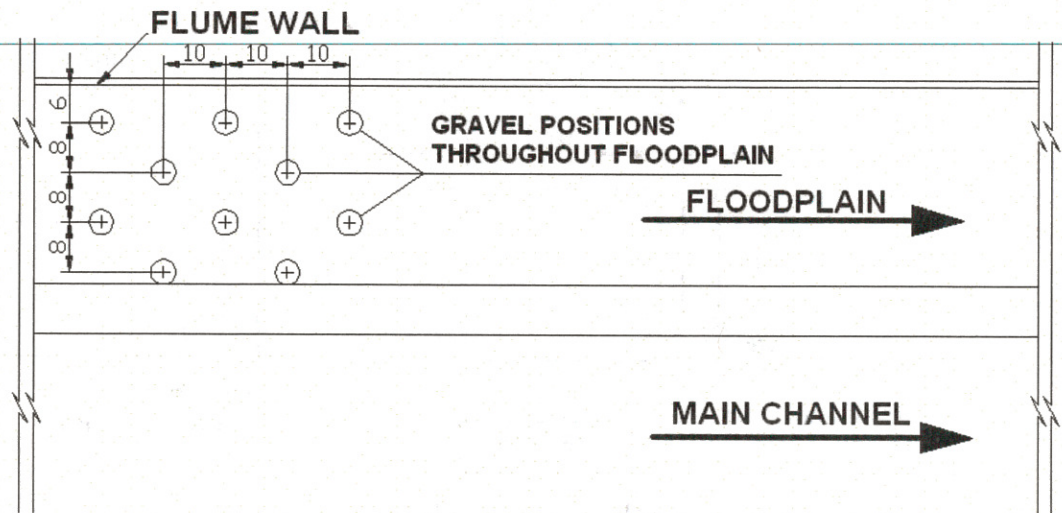


Figure 4-3: Scheme of staggered placement of gravel on floodplain to provide roughness. Gravel was placed throughout the floodplain (cm).

6.1 The Abutment Model

The wing-wall abutment model was made of sheet steel. The dimensions of the model are shown in Fig. 4-4. The abutment terminated on the bank slope of the main channel as illustrated in Fig. 4-1, which corresponds to the Type III abutment of Melville (1992). The height between the top of the floodplain and the top of the abutment was 60 mm. The abutment length was about 1/3 of the channel width and was observed not to alter the flow enough to interact with the far flume wall.

6.1 Sediment Characteristics

The bed material sediment used in the main channel had a diameter of 0.8 mm. The standard deviation of the sediment diameter, σ_g , $[\sigma_g = (D_{84} / D_{16})^{1/2}]$, was equal to 1.37. According to a modified version of Shields diagram (Miller et al., 1977), the critical shear velocity of the bed sediment is 1.995 cm/s. In live-bed conditions, the sediments were circulated with the water by the pump. At the upstream inlet of the flume a gradual-transition contraction was built to guide the sediment into the main channel.

$$\frac{U_c}{u_{*c}} = 5.75 \log\left(\frac{Y_o}{k_s}\right) + 6.0 \quad (4-2)$$

So for clear-water conditions, where the bed is stable and k_s is constant,

$$\frac{U}{U_c} = \frac{u_*}{u_{*c}} \quad (4-3)$$

For our experiments,

$$u_{*c} = 1.995 \text{ cm/s} = 0.01995 \text{ m/s},$$

Setting $\frac{U}{U_c} = \frac{u_*}{u_{*c}} = 0.9$ for clear-water scour, then

$$u_* = 0.017955 \text{ m/s}$$

Since

$$u_* = \sqrt{gRS} \quad (4-4)$$

If flow depth is set, the slope of the flow should be able to be determined. U and U_c can also be determined by selecting $k_s = 2D_{50} = 1.6 \text{ mm}$.

Three flows were used with velocity ratios (U/U_c , where U is the average velocity of the flow and U_c is the critical velocity for incipient motion for the bed material) of 0.9, 1.5, and 2.3. The critical velocity of the bed material was calculated using the velocity distribution relation for a rectangular cross-section, rough wall, and free surface as shown in Equation (4-2) above.

For clear-water conditions ($U/U_c = 0.9$), the experiments were run for 4800 minutes so that the local scour had reached a near equilibrium value. For live-bed conditions ($U/U_c = 1.5$ and 2.3), all experiments were run for 3000 minutes to assure that at least 125 bed forms migrated past the abutment.

6.1 Instrumentation

7. Set the predetermined flume slope and start the pump.
8. Adjust the pump speed to obtain uniform flow at the selected flow depth using the point gages by measuring the water surface elevation at both ends of the 12-m transect in the center of the channel. Check further the water surface slope along the 12-m transect using the RMU device to ensure the uniformity of the flow. Maintain the same rate of flow and approach depth for the entire experimental run.
9. Collect transects of the scour region at 30 min intervals. Increase this time interval to 60 min to 90 min or more as the experiment progresses and changes in the scour region become slower.
10. Continue the experiment until the changes in the scour hole become very slow (approximately 80 hours).
11. Stop the pump, dewater the flume carefully and contour the scour hole.
12. Take a photo of the scour hole.

6.3.2 Discussion of Clear-water Baseline Experimental Results

5.1.2.1 Scour pattern

Two scour patterns were discovered depending upon the difference of the roughness on the floodplain. Without gravel on the floodplain the scour pattern of Fig. 5-1 occurred in which there were five scour locations. Tests B1 ~B4 (not roughened with gravel) had similar scour patterns. The first scour hole, Zone A, was at the upstream corner of the abutment and posed the greatest threat to the stability of the abutment. Scour in Zone B was located some distance away from the abutment face in the bridge crossing and was where the maximum scour hole was located. Since it was away from the abutment, it was considered to not threaten the abutment. Scour in Zone C was a short distance downstream of the abutment. This scour zone may pose a threat to the main channel bank immediately downstream of the abutment. Scour in Zone D was far out into the main channel and, therefore, posed no threat to the abutment. Scour in Zone E was located at a short distance upstream of the abutment corner and seemed to be the initial part of Scour Zone B. With gravel on floodplain Test B5 had a slightly different scour pattern as shown in Fig. 5-2, where scour Zones A, B and E merged to be the maximum scour location and was located at the upstream corner of the abutment.

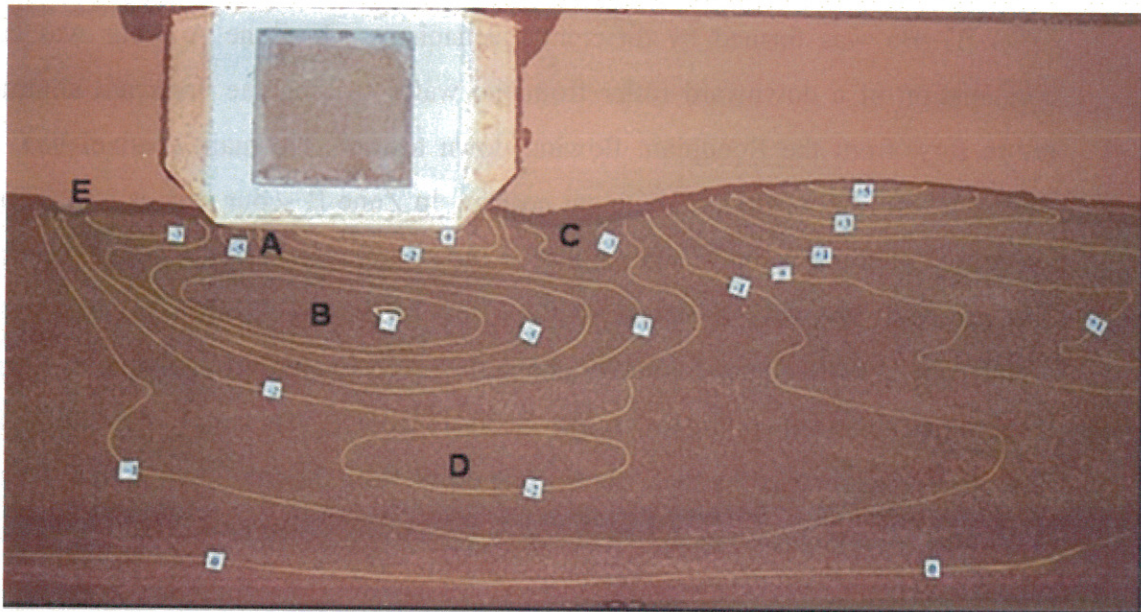


Figure 5-1: String contour of baseline Test B3. Flow is from left to right.

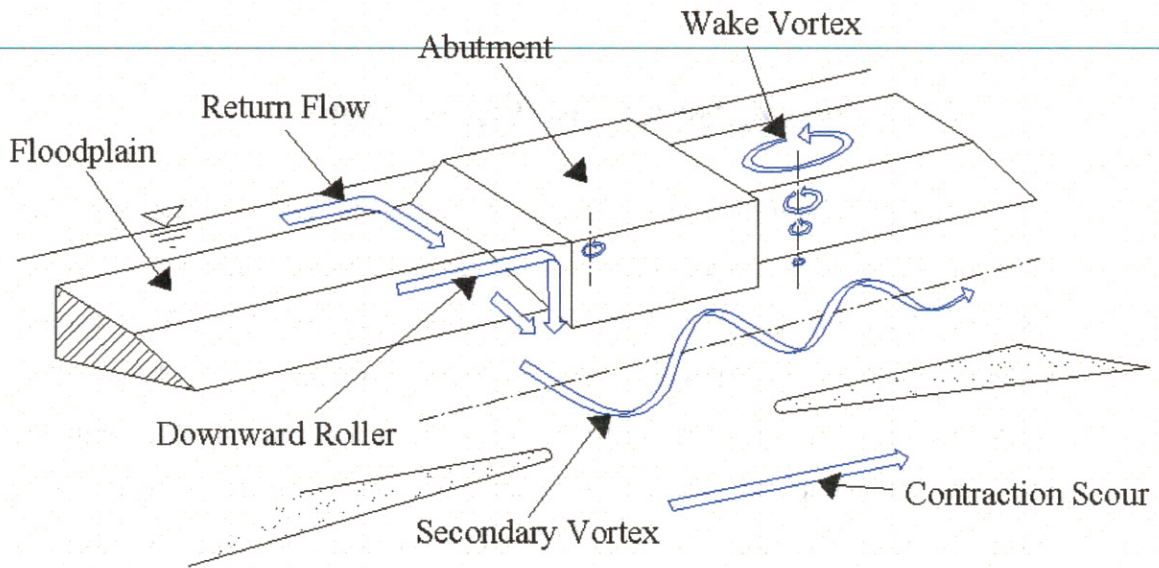


Figure 5-3: Flow patterns around a wing-wall abutment. Flow is from left to right.

5.1.2.3 Effect of Floodplain Roughness on Scour Depth at Upstream Corner of the Abutment

The mechanisms of the formation of the four scour holes in Test B1~B4 were explained above. Also, it was seen that the maximum scour depth was found in the bridge crossing a distance away from the abutment instead of being at the upstream corner of the abutment. It then was hypothesized that the reason the maximum scour depth was not located right at the upstream corner of the abutment was because the velocity ratio between the floodplain flow and the main channel flow was so high that the floodplain flow was able to jet into the main channel a distance away in front of the abutment instead of being fully confined around the abutment corner. To solve this problem with the hope of the maximum scour depth taking place right at the upstream corner of the abutment, the floodplain was further roughened with gravel of average diameter 4.5 cm as shown in Fig. 4-2. As was expected, the result in Fig. 5-2 showed that the scour in Zones A, B and E merged and the maximum scour hole was found right at the upstream corner of the abutment.

downstream scour holes (C in Figure 5-1 or Figure 5-2) because the strength of the vortex systems at the upstream corner of the abutment were generally stronger than those at the downstream end of the abutment. Therefore, the upstream scour hole reaches equilibrium quicker than the downstream scour hole. Depending on the height of the main channel bank and flow conditions, the depth of the downstream scour hole may or may not be greater than the scour depth at the upstream corner of the abutment. Figures 5-4 and 5-5 show the evolution of the scour depths of both the upstream and downstream scour holes with time for Test B1 and B4, respectively.

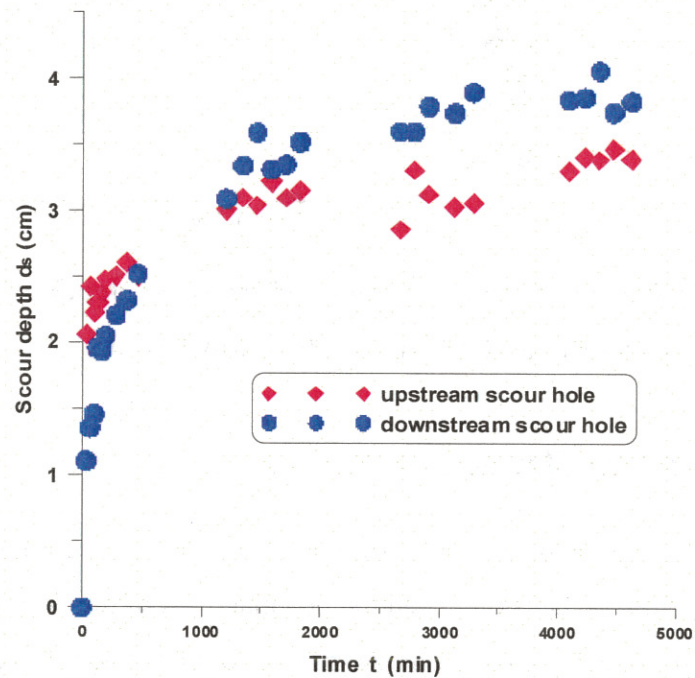


Figure 5-4: Plot of the time evolution of the scour depth of both the upstream (A) and downstream (C) scour hole at the abutment in Test B1.

abutment without any countermeasures should be determined first as a reference. The live-bed baseline scour results were obtained under the flow conditions shown in Table 5-2.

Table 5-2. Experimental results for baseline scour depth for three velocity ratios.

Velocity ratio U/U_c	Flow depth in main channel y_m (cm)	Flow depth in flood plain y_f (cm)	Total discharge Q (m ³ /s)	Run time, t (min)	Time-averaged baseline scour depth $d_{abut,avg}$ (cm)	Instantaneous maximum scour at abutment $d_{max,abut,inst}$ (cm)
0.9	13.2	5.2	0.0387	4800	7.77	7.77
1.5	13.2	5.2	0.0622	3000	7.23	15.00
2.3	13.2	5.2	0.0966	3000	7.52	17.28

In the live-bed condition, due to the wavy water surface and the fast moving and fluctuating bed forms, velocity profile measurements turned out to be difficult. Therefore, the flow was mainly controlled by the discharge and the average water surface profile and the average bed profile along a 12-m transect in the middle of the approach channel. First the discharge was set to be 1.5 times the discharge at the critical condition, and then the slope was adjusted until the average water surface slope and average bed surface slope are equal to the flume slope, i.e., the uniform live-bed flow condition through trial and error. The flow depth was also adjusted to be 13.2-cm deep as it was in the clear-water case.

Also, due to the fast change of the bed profiles at the bridge crossing, it is impractical to measure the bed profile as it was done in clear-water scour condition, which took 14 transects and more than 13 minutes to cover the whole scour region as well as each point once. Therefore, in this case, only one 2.5 m long transect at the main channel side of the abutment was chosen to monitor the time evolution of the scour at the edge of the abutment. This transect starts from a point 1.5 m upstream of the upstream abutment tip and travels parallel to the flow just to the right of the abutment. Each loop of the transect takes 54.90 seconds and a total of 133 loops is set to capture the local scour as well as the bed forms

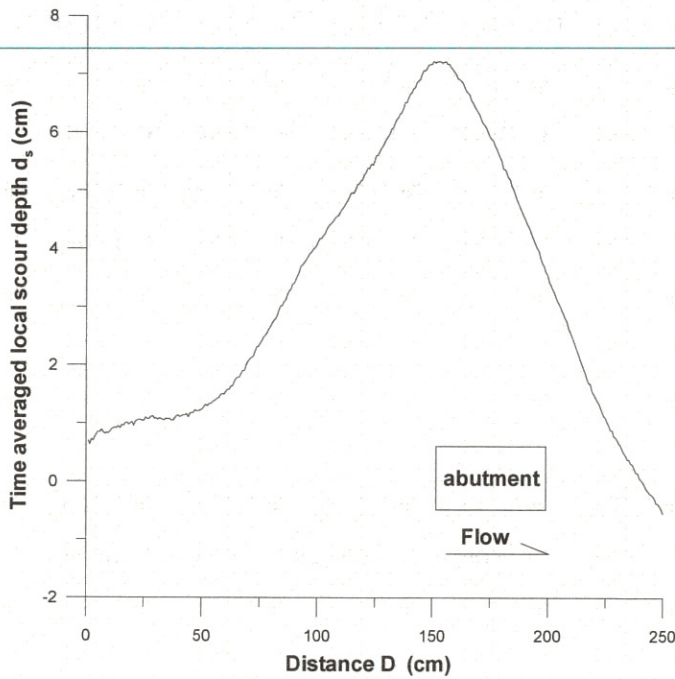


Figure 5-6: Time-averaged local scour depth along the 2.5-m transect at the abutment versus distance starting from a point 1.5 m upstream of the upstream abutment corner.

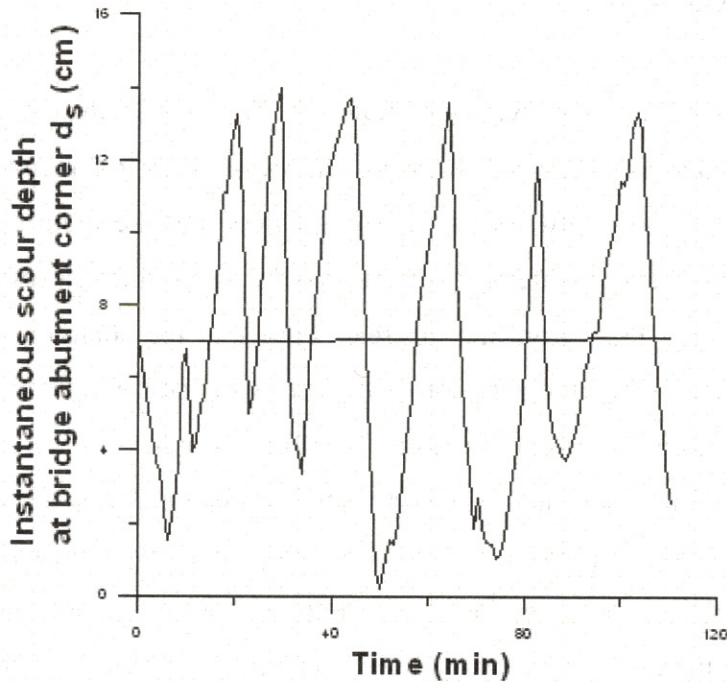


Figure 5-7: Time evolution of baseline scour at the upstream abutment corner after equilibrium was reached.

3. The principal vortex systems and secondary vortex systems at the upstream corner of the abutment were stronger than the wake vortex systems at the downstream corner of the abutment. Consequently, the scour hole induced by the principal vortex systems and the secondary vortex systems reaches equilibrium quicker than the scour hole induced by the downstream wake vortex systems.
4. Test B5 will be used as the clear-water baseline condition for following countermeasure experiments with a scour depth of 7.77 cm as a reference.

Under live-bed conditions:

1. Maximum scour took place at the upstream corner of the abutment. Time-averaged scour depth at the upstream corner is less than the scour depth under critical clear-water condition, while instantaneous scour depths were between values near zero to values nearly twice the maximum scour under clear water flows because of the superposition of the trough of bed forms (Figure 5-7);
2. Live-bed scour reaches equilibrium quicker than clear-water scour.

Results in Table 5-2 will be used as the references to evaluate the efficiency of countermeasures that will be tested later.

guide bank can be designed such that the slope of the guide bank is tangent to the slope of the abutment and there is no protrusion of the abutment into the flow beyond the slope of the guide bank. However, in a wing-wall case, this point may not be achieved readily because of the vertical front faces of the abutments. In this situation either the slope of the guide bank protrudes out beyond the abutment face or the abutment face protrudes out beyond the guide bank slope. The impacts of these configurations on local scour at abutments need to be studied. Another issue is that a careful review of those guidelines (Bradley 1978) for determining the length of guide banks shows that they were designed for spill through abutments in wide floodplain rivers and they may not apply to smaller county bridges. There are many gray areas that were not addressed and may be important for small county bridges. For instance, first, it is recommended that if the length read from the design chart is less than 9.1m (30 ft), a guide bank is not needed. This might not be true for a small two lane bridge whose width is about 9 m and a 9 m long guide bank may make a great difference in protecting the bridge abutments; second, it is recommended that for chart lengths from 9 m to 30 m, a guide bank no less than 30 m long be constructed. However, according to Herbich (1967), the length of the guide banks appear to be unimportant in reduction of velocities provided it is greater than a certain minimum length. Therefore, an unnecessarily long guide bank may increase the cost of the structure and not improve its effectiveness. Yet another issue is that the parameters defined and used in determining the length of guide banks may not be easily available. For instance, the total stream discharge, Q , the lateral or floodplain flow discharge Q_f and the discharge in the 100 feet of stream adjacent to the abutment, Q_{100} (Bradley, 1978). In addition, in spite of the fact that an elliptical-shaped end seems to be favorable by all design recommendations because the curved head can direct the flow smoothly into the main channel and reduce scour at the guide bank end, for small county rivers and streams whose floodplains are relatively narrow and are mostly farmlands under cultivation, the floodplain flow velocity may be relatively low and a curved head may not be justified. Most importantly, for those abutments terminating on the riverbanks, a curved end stretching out from the bank into the farmland may be aesthetically and practically not acceptable. This chapter deals with design issues for parallel walls on small rivers with wingwall abutments. These parallel walls are essentially scaled-down and simplified versions

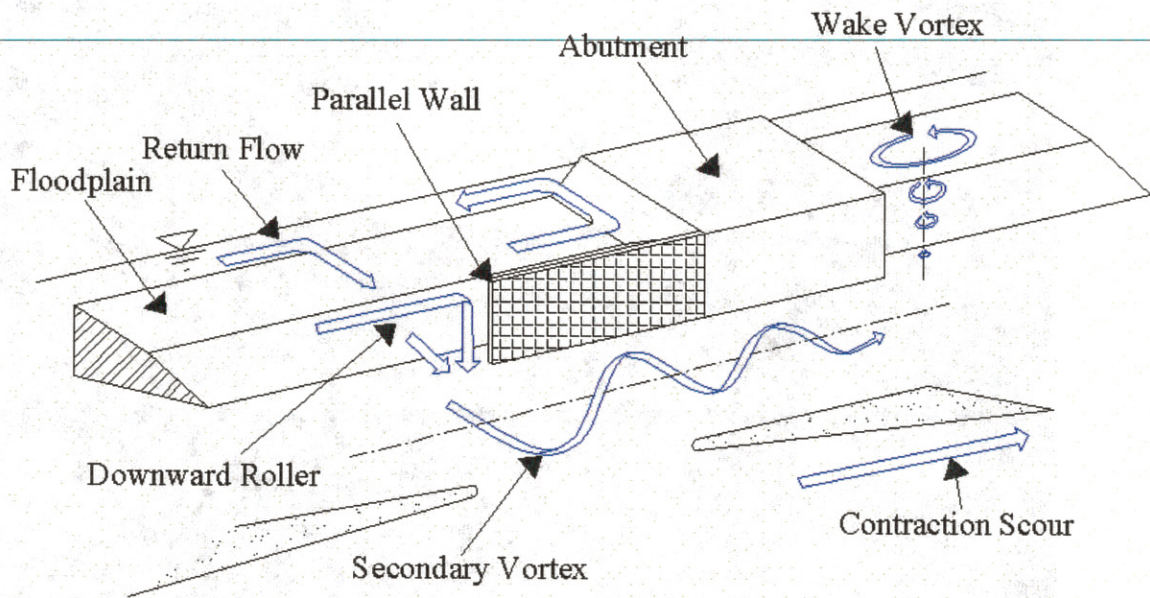


Figure 6-1: A sketch of the conceptual model of parallel wall as countermeasure against abutment scour in a compound channel.

6.3 Results

6.3.1 Solid Parallel Wall

A series of rectangular solid walls made from 13-mm thick plywood of different lengths, L_s , attached to the upstream end of the abutment and parallel to the flow direction were tested (Fig. 6-1). Solid walls are tested because in certain areas rocks may be not readily available and cost efficient. All the solid parallel walls were seated at the bottom of the bank slope and aligned with the abutment face parallel to the flume wall. The top of each wall was the same height as the top of the abutment except in one clear-water case, in which the wall height was 5.2 cm lower than the water surface. In these cases, the flow depth on the floodplain, y_f was equal to 5.2 cm and the flow depth in the main channel, y_m , was 13.2 cm. The velocity ratio U/U_c was about 0.9, 1.5 and 2.3 in the center of the entire channel for each of the three flow conditions tested. Table 6-1 gives results of the solid wall experiments under clear-water conditions and Table 6-2 gives results under live-Bed conditions. Figure 6-2 is a string contour of the 1.2L solid wall run in

Table 6-2: Solid wall experimental results for live-bed scour (run time=3000 min., $Q=0.0619 \pm 0.0015\text{m}^3/\text{s}$ for $U/U_c=1.5$, and $Q=0.0619 \pm 0.0015\text{m}^3/\text{s}$ for $U/U_c= 2.3$, all walls were rectangular shaped and emergent).

L_s	U/U_c	$d_{\text{abut,avg}}$ (cm)	$\%_{\text{max,abut, avg}}$	$d_{\text{max,abut,inst}}$ (cm)	$\%_{\text{max,abut,inst}}$	$d_{\text{cm,avg}}$ (cm)	$d_{\text{max,cm,inst}}$ (cm)
0.6L	1.5	5.05	30	12.98	13	7.57	14.36
0.9L	1.5	4.04	44	9.56	36	7.9	15.86
1.2L	1.5	2.57	63	10.12	33	7.74	13.81
1.5L	1.5	0.22	92	5.49	63	7.86	14.20
1.6L	2.3	2.23	70	8.84	49	9.21	16.43
1.9L	2.3	3.57	53	8.94	48	9.82	16.73

L_s = wall length, U = average velocity in main channel, U_c = critical velocity for sediment movement, $d_{\text{abut,avg}}$ = time-averaged scour depth at abutment, $\%_{\text{max,abut, avg}}$ = percent reduction in time-averaged scour depth at abutment, $d_{\text{max,abut,inst}}$ = maximum instantaneous scour depth at abutment, $\%_{\text{max,abut,inst}}$ = percent reduction in maximum instantaneous scour depth at abutment, $d_{\text{cm,avg}}$ = time-averaged scour depth at the countermeasure, $d_{\text{max,cm,inst}}$ = maximum instantaneous scour depth at the countermeasure

clear-water scour where $y_m = 13.2$ cm, $y_f = 5.2$ cm, $Q = 0.0379$ m³/s, time = 4800 minutes. Flow is from left to right. Contour interval is 1 cm.

6.3.2 Discussion of Solid Wall Length

Fig. 6-3 is a plot of the maximum scour depths at the abutment and the maximum scour depth in the vicinity of the upstream end of the wall versus the length of the wall in terms of the abutment length, L , for both clear-water ($U/U_c = 0.9$) and live-bed ($U/U_c = 1.5$) experiments. It is seen that, as the length of the wall increases from 0.3L to 1.2L, the scour at the abutment decreases rapidly. There is no scour at the abutment corner in 4800 minutes of running when the wall reaches a length of 1.1L.

maximum contribution from the bed forms to the scour depth varies from 7.93 cm to 4.91 cm. It can be seen that although increases in solid wall length decreased the amplitude of the bed forms, the decreases are not significant, which implies that if the height of bed forms constitutes a large part of the local instantaneous scour depth, it can only be completely eliminated when the presence of the solid wall happens to be able to change the flow condition in the bridge crossing into a transition regime under which the dunes completely disappear and a flat bed with bed material transport is formed. This transition regime may or may not be readily achieved depending on the approach flow conditions and the constriction ratio of the channel.

It was also found from the live-bed experimental data with a velocity ratio of 2.3 that when the length of the wall was increased from 1.6L to 1.9L, the scour reduction rate at the abutment decreased from 70 percent to 53 percent instead of being increased. This may be due to imperfect construction of the floodplain or wall, or it may be that these two scour values are within the range of scatter of the scour data for this high-sediment-transport flow.

In summary, it was found that, in general, walls attached to the upstream end of the abutment were able to move the scour hole upstream from the abutment corner and therefore, were effective as a scour countermeasure. It was also found that, for clear-water scour conditions, as the length of the wall increased, the scour at the abutment declined. In live-bed experiments, however, when the length of the wall becomes longer than a certain length, the scour at the abutment begins to increase.

6.3.3 Parallel Rock Wall Experimental Results

A series of rock walls of different lengths, L_w , and different protrusion lengths, L_p , were tested (Fig. 6-4) both under clear-water and live-bed conditions. This design was thought to be easier to construct in the field and less expensive than a solid wall. In these experiments, the flow depth on the floodplain (y_f) was equal to 5.2 cm and the flow depth in the main channel (y_m) was 13.2 cm. The velocity ratio (U/U_c) was 0.9 in the centerline of the entire channel for clear-water experiments and 1.5 and 2.3 for live-bed experiments,

Table 6-3: Experimental data of parallel rock walls in clear-water scour ($Q = 0.0385 \pm 0.003\text{m}^3/\text{s}$, $t = 4800 \text{ min.}$, $U/U_c=0.9$).

Test No.	Gravel diameter D (mm)	Wall length, L_w (L)	Side slope, S_b	End slope, S_n	Wall protrusion, L_p (W)	Maximum Scour at Abutment, d_s (cm)	Scour Reduction (%)
1 (Fig. 6-5)	6.7~9.5	1.5	18/13.2	30/13.2	0.5	0.2	97
2	6.7~9.5	0.5	18/13.2	30/13.2	0.5	5.21	29
3	6.7~9.5	1.0	18/13.2	30/13.2	0.5	5.06	35
4 (Fig. 6-6)	6.7~9.5	1.5	18/13.2	30/13.2	0.25	0.45	94
5	6.7~9.5	0.5	18/13.2	30/13.2	0.25	5.3	32
6	6.7~9.5	1.0	18/13.2	30/13.2	0.25	2.35	70
7 (Fig. 6-7)	6.7~9.5	1.5	18/13.2	30/13.2	0	1.9	76
8	6.7~9.5	1.0	18/13.2	30/13.2	0	1.95	75
9	6.7~9.5	0.5	18/13.2	30/13.2	0	2	74
10	6.7~9.5	0.25	18/13.2	30/13.2	0	2.8	64
11	6.7~9.5	2.0	18/13.2	30/13.2	0	2	74
12	19~50	1.5	18/13.2	30/13.2	0	0.3	96

From Tests 1(Fig. 6-5), 2, and 3 in Table 6-3 it was found that with a protrusion length of the wall base of $0.5W$ beyond the abutment face into the main channel, there tended to be a separation zone behind the downstream end of the wall, causing a significant local scour hole. When the length of the wall was $1.5L$, the scour hole was relatively small (8.81 cm) and did not pose a direct threat to the abutment. However, when the length of the wall was $0.5L$, the scour holes were 12.96 cm and the abutment was highly threatened. These scour holes could pose significant threat to a pier if a pier is located near the abutment.

Table 6-4: Rock wall experimental results in live-bed scour (run time=3000 min., $Q=0.0619 \pm 0.0015\text{m}^3/\text{s}$ for $U/U_c=1.5$, and $Q=0.0966 \pm 0.003\text{m}^3/\text{s}$ for $U/U_c= 2.3$, all walls were rectangular shaped and emergent).

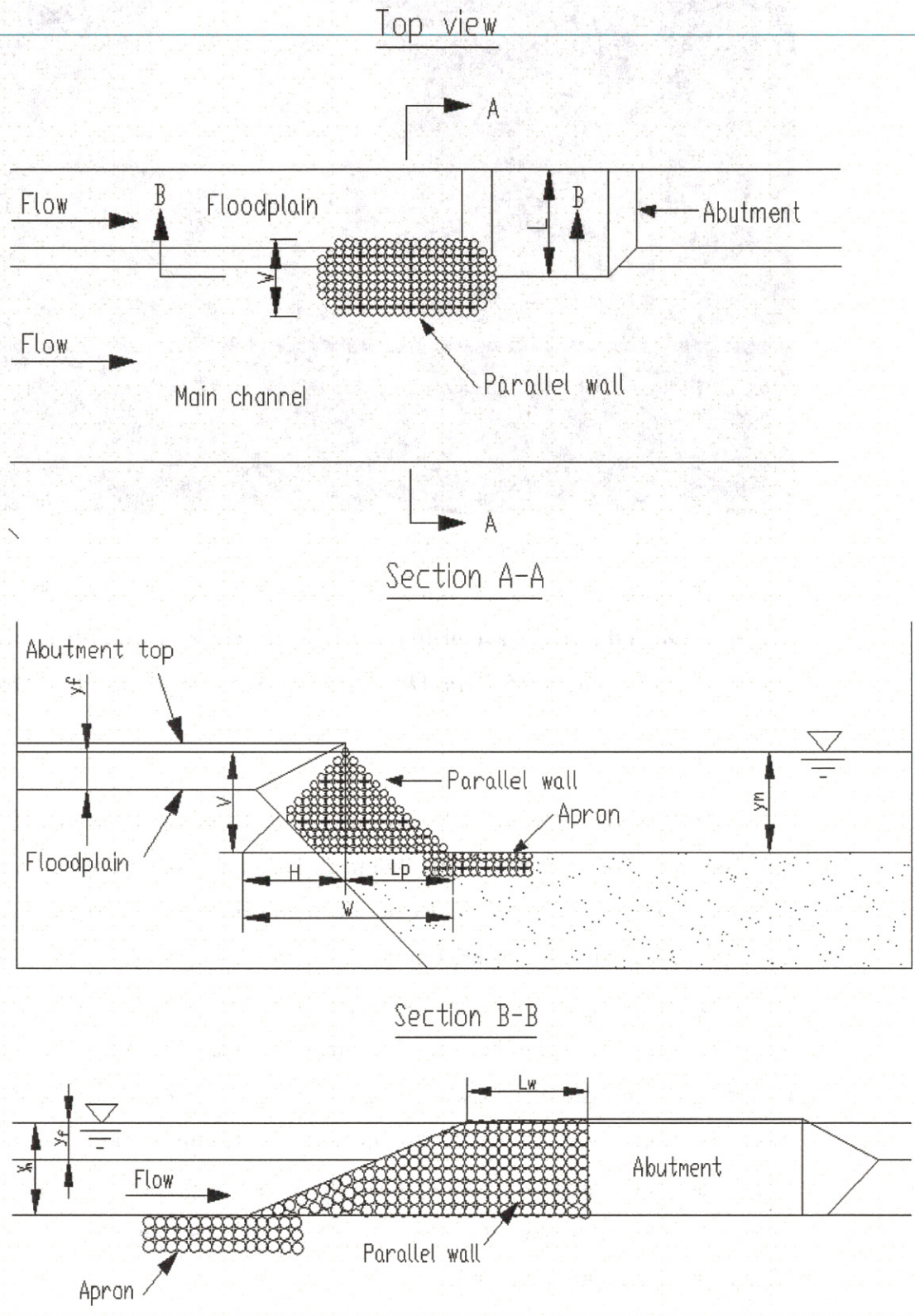


Fig. 6-4: Definition sketch of parallel wall (aprons were only present in live-bed experiments).

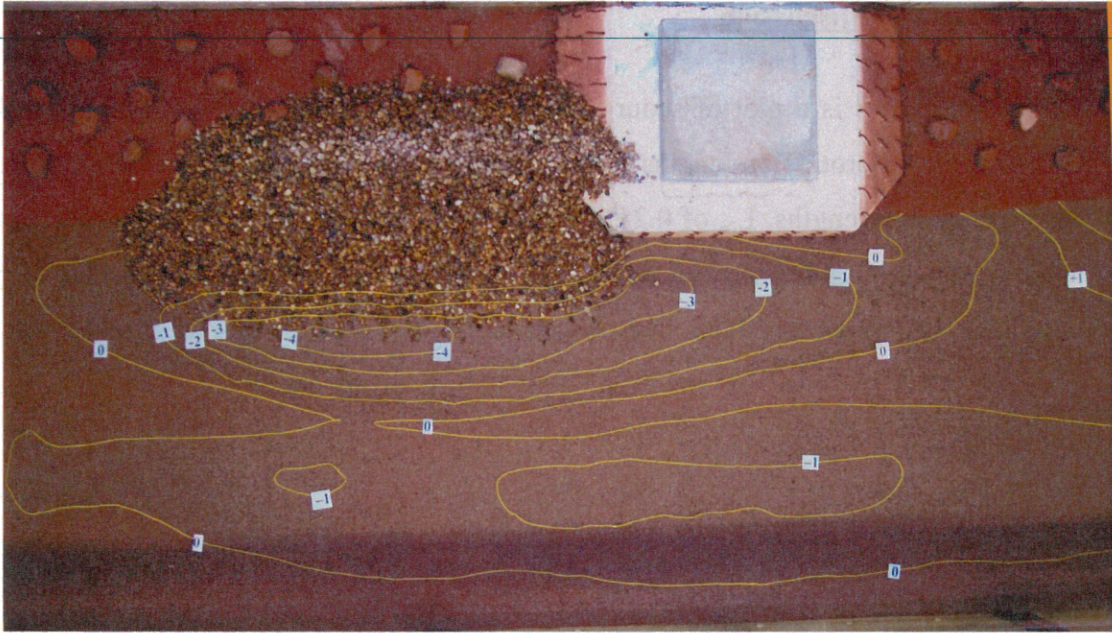


Fig. 6-6: Scour contour of test No 6. in Table 4 with gravel diameter 6.7~9.5 mm, 1.5L length, rock wall end slope H:V=30/13.2, side slope H:V=18/13.2, a small apron at the end . Wall base protruded out into main channel from abutment a quarter wall width. $y_m = 13.2$ cm, $y_f = 5.2$ cm, $Q = 0.0373$ m³/s, $t = 4800$ min. Flow from left to right.



Fig. 6-7: Scour contour of Test 9. in Table 6-3 with gravel diameter 6.7~9.5 mm, 1.5L length, rock wall end slope H:V=30/13.2, side slope H:V=18/13.2, a small apron at the end . Wall base is even with abutment. $y_m = 13.2$ cm, $y_f = 5.2$ cm, $Q = 0.0371$ m³/s, $t = 4800$ min. Flow from left to right.

seen from this plot that for the 0.25W and 0.5W protrusion lengths, increases in wall lengths can significantly reduce the maximum scour depth that is induced by the presence of the walls. While for walls with protrusion length of zero, increases in wall length result in essentially no reduction in scour depth (i.e. scour at abutment) when wall lengths are greater than 0.5L.

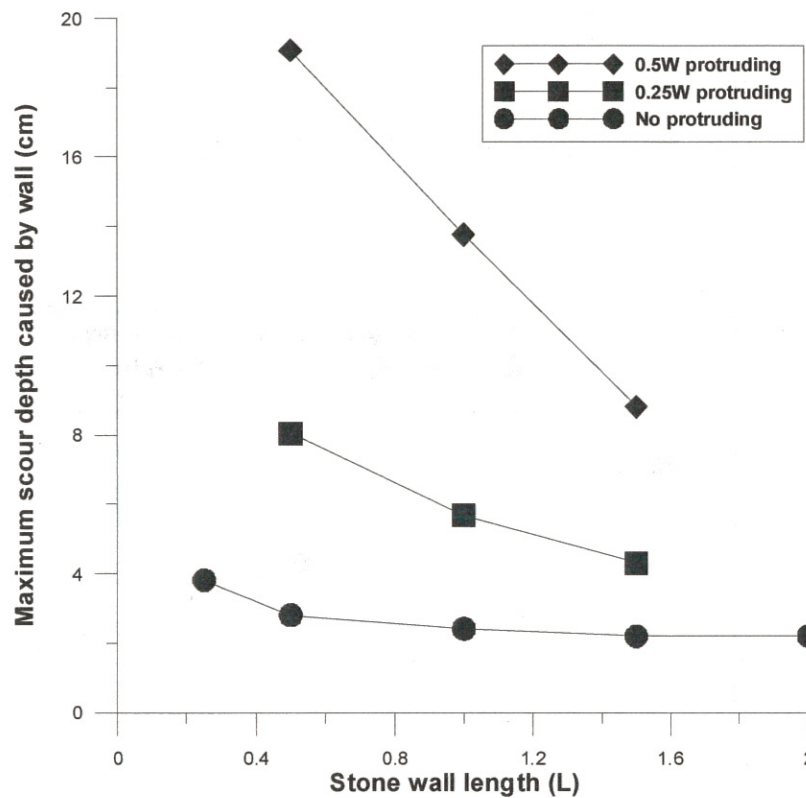


Fig. 6-9: Plot of the maximum scour depth caused by the wall in the entire channel versus rock wall length for different wall protrusion lengths under clear-water conditions ($U/U_c=0.9$).

Fig. 6-10 is a plot of both time-averaged and maximum instantaneous scour depth at the bridge abutment versus rock wall length for zero protrusion length under live-bed conditions. The time-averaged scour depth was calculated by measuring the scour depth at regular time intervals and then averaging over time. It gives a sense of the average depth of scour. The maximum instantaneous scour depth is the maximum scour measured at any time in the scour time series data collected. Even though this maximum scour value would not

effective in protecting the abutment, (2) walls whose base protruded into the main channel beyond the abutment (protrusion length, $L_p=0.25W$ or $0.5W$) tended to produce significant scour in the bridge crossing and potentially threaten the middle and downstream abutment end while the length of these walls became shorter than a certain length, and (3) for zero protrusion length, $L_p=0$, the scour protection of the walls was not sensitive to the lengths of the wall unless it was less than $0.5L$. Below this length the degree of scour protection decreased.

Regarding the amount of mass transfer or water flow through the rock wall itself, during the experiments, dye was injected in the floodplain side of the parallel walls. For all of the flow conditions investigated, no significant amount of dye was observed to flow through the rocks. This indicated that there is no significant flow transfer through the wall. In addition, an $0.8L$ long parallel solid wall with 85 circular holes with 8 mm diameter uniformly distributed on the wall was tried and compared with the $0.8L$ impermeable wall. The result was quite similar. This showed that when the permeability of the wall is smaller than a certain value, the solid wall acts like an impermeable one.

Cases of clear-water and live-bed scour were investigated. It could be that during flow conditions in which there was less downstream velocity, that there is more flow through the wall. This would most likely not be critical for scour, however, since clear-water and live-bed scour are the two worst cases for scour.

In all of the experiments reported on here, there was no gap between the countermeasure and the abutment. Care should be taken to ensure this, as a high-velocity jet may form if such a gap existed, that could exacerbate the scour depth in unknown ways.

6.4.3 Height and Width of Wall Crest

Heights for both solid wall and parallel rock wall should be at least as high as the bottom height of the lowest bridge deck so that flow can not enter the bridge crossing at the abutment even in the worst case scenario.

The width of a solid wall depends on the construction material used. It could be a several centimeters if a steel plate is used. The width of a parallel rock wall crest need not be larger than one stone diameter.

6.4.4 Slope of Wall and Apron

The side slope of the rock wall must be less than the rock's angle of repose to insure stability. However, the side slope should be as high as possible so that the protrusion of the abutment beyond the wall slope is the minimum. It is recommended that the side slope of the wall be about 5 degree less than the angle of repose of the rocks. The slope at the upstream end of the wall can be much flatter than the side slope to help stabilize the end of the wall and reduce local scour there. Therefore, an end slope of 2~2.5:1(H:V) is preferred.

Aprons are always needed at both the bottom of the side slope and the upstream end slope so that when scour takes place at those spots aprons can launch to prevent sliding of rocks from both slopes. Thickness, area limit and relative position with the parallel rock wall should be determined according to the scour depth and position of the scour hole along the wall.

6.4.5 Comparison of Solid and Rock Parallel Walls

If the best designs for both solid wall and rock wall are compared, it can be seen that the rock walls have advantages over the solid wall. Table 6-5 shows scour depths for both solid and rock walls for both clear-water and live-bed scour conditions. It can be seen that the rock wall allows less scour at the abutment than the solid wall. The solid wall, therefore, seems to be feasible only when the cost of rocks is prohibitively high.

CHAPTER 7. SPUR DIKE AS AN ABUTMENT SCOUR COUNTERMEASURE

7.1 Introduction

Scour at bridge crossings can cause damage or failure of bridges and result in excessive repairs, loss of accessibility, or even death. Mitigation against scour at bridges has received much attention in the past few decades. Hydraulic countermeasures against bridge abutment scour can be classified as river training structures and armoring countermeasures. Considerations in choosing the appropriate method of mitigation include maintenance and inspection requirements, enhancement of the physical environment, and construction methods needed other than design constraints. Design specifications for many of these scour mitigation techniques can be found in Lagasse et al., 2001.

Spur dikes, the focus of this paper, have been used extensively in all parts of the world as river training structures to enhance navigation, improve flood control, and protect erodible banks (Copeland, 1983). Spur dikes are structures that project from the bank into the channel. They may be classified based on their permeability: high permeability - retarder spur dykes; impermeable - deflector spur dikes; and intermediate permeability - as retarder/deflector (Brown, 1985). They may be constructed out of a variety of materials including masonry, concrete, earth and rock, steel, timber sheet piling, gabions, timber fencing, or weighted brushwood fascines. They may be designed to be submerged regularly by the flow or to be submerged only by the largest flow events.

A spur dike serves one or more of the following functions.

- (1) Training of the stream flow. For instance, spur dikes are commonly used to realign streams as they approach a bridge abutment. A bridge abutment may be in danger of being severely eroded when it is subjected to high velocity flow from a channel that has changed course due to meandering.
- (2) Protection of the stream bank (may or may not contain bridge abutments) from erosion.



Fig. 7-1: Photograph of excessive scour around a poorly-positioned spur dike. (Flow from left to right.)

7.2 Conceptual Model

Figure 7-2 is a sketch of the conceptual model of a spur dike as a countermeasure against abutment scour in a compound channel. A spur dike is placed a certain distance away upstream of the abutment and is perpendicular to the flow direction. Flow on the floodplain can only go around the main channel end of the spur dike. A spur dike thus installed is expected to be able to block the floodplain flow from hitting the abutment face and direct the flow into the main channel. It may create wake vortices behind itself. The effects of these wake vortices and scour hole at the spur dike structure on the abutment scour should be evaluated experimentally to determine the best configuration of spur dikes as countermeasures. In the following experimental studies, number of spur dikes, distance between spur dikes and distance between spur dike and abutment, protrusion length, and construction material of spur dikes will be tested as parameters.

Table 7-1: Preliminary Solid Spur Dike Experimental Results ($Q=0.0387 \pm 0.003\text{m}^3/\text{s}$, $U/U_c=0.9$, $y_m = 13.2 \text{ cm}$, $y_f=5.2 \text{ cm}$).

Ru n No.	Spur dike description notes	L_s (L)	D_s (L)	θ (deg)	t (min)	$d_{\text{abut.avg}}$ (cm)	$\%_{\text{max,abut, avg}}$ (%)	$d_{\text{max.sp.avg}}$ (cm)
Sp-1	Rectangular , protrusion length equal to the width of floodplain	0.7	2	90	1254	4.52	32.2	--
Sp-2		1	2	90	1540	4.60	34.8	10.52
Sp-3	Fig. 6	0.7	1	45	4800	4.69	39.6	14.40
Sp-4		0.7	1.5	45	1685	4.50	35.2	13.90
Sp-5	Fig. 7	0.7	1.5	45	1440	4.33	36.5	13.53
Sp-6	Fig. 8	1	0.58	90	2580	5.80	20.6	--

Note: L_s = Spur dike protrusion length; D_s = distance between the farthest spur dike tip at the main channel end and abutment tip; θ = Spur dike orientation angle with respect to the flow; t = Run time; $d_{\text{abut.avg}}$ = Time averaged scour depth at abutment; $\%_{\text{max,abut, avg}}$ = Percent of scour reduction; $d_{\text{max.sp.avg}}$ = Maximum scour depth at spur dike.

The flow-perpendicular length of spur dike was found to be an important variable in protecting the abutment. Flow-perpendicular lengths were restricted to the length of the abutment or less in this experimental series to prevent contraction of the flow in the main channel. The six cases tested show that spur dikes of the same flow perpendicular length as the abutment do not protect it from scour regardless of spacing or orientation angle (Figs. 7-3, 4 and 5). When the spacing (D_s) of the spur dikes was less than the flow perpendicular length of the abutment (L), the upstream corner of the abutment will fall into the scour hole induced by the spur dike (Fig. 7-5). When the spur dikes were far away ($D_s \geq 1.5L$) from the

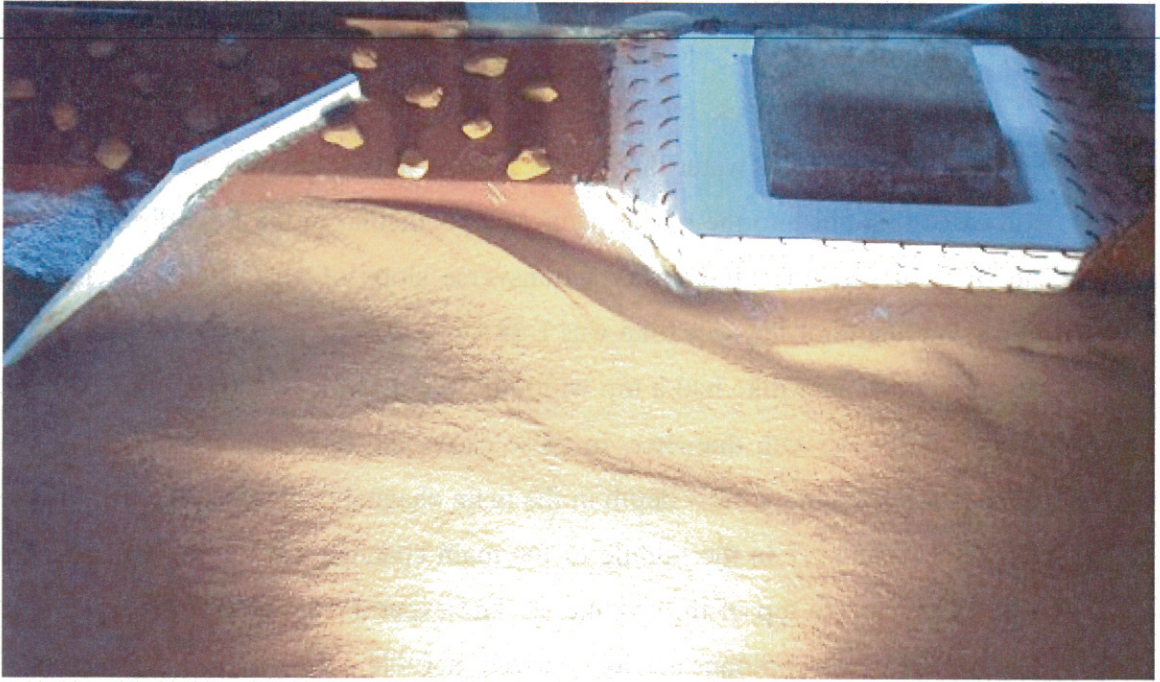


Fig. 7-4: Photograph of Sp-5. Flow from left to right.



Fig. 7-5: Photograph of Sp-6. Flow from left to right.

Table 7-2: Clear-water experimental data of rock spur dikes ($Q = 0.0368 \pm 0.0016 \text{ m}^3/\text{s}$, $U/U_c = 0.9$, $y_m = 13.2 \text{ cm}$, $y_f = 5.2 \text{ cm}$, gravel diameter $D = 6.7 \sim 9.5 \text{ mm}$, running time $t = 4800 \text{ min}$, all spur dikes had a top protrusion length of $1.0L$, a bottom protrusion length of $1.5L$, and end slope of $H:V=22/13.2$).

Run No.	n	$D_s, (L)$	$d_{\text{abut.avg}}$, (cm)	$\%_{\text{max, abut}}$	$d_{\text{max.sp1.avg}}$, (cm)	$d_{\text{max.sp2.avg}}$, (cm)	$d_{\text{max.sp3.avg}}$, (cm)
Sp-7 (Fig. 7-6)	2	1	0	100	8.75	11.00	--
Sp-8 (Fig. 7-7)	3	1	0	100	7.62	6.61	7.71
Sp-9 (Fig. 7-8)	3	2	2.00	74.3	13.14	3.50	6.89
Sp-10 (Fig. 7-9)	2	1	0	100	7.56	10.30	--

Note: n = number of spur dikes; D_s = Spacing between spur dikes or spur dike and abutment; $d_{\text{abut.avg}}$ = Time averaged scour depth at abutment; $\%_{\text{max, abut}}$ = Percent of scour reduction; $d_{\text{max.sp1.avg}}$ = Maximum scour depth behind the first spur dike; $d_{\text{max.sp2.avg}}$ = Maximum scour depth behind the second spur dike; $d_{\text{max.sp3.avg}}$ = Maximum scour depth behind the third spur dike.

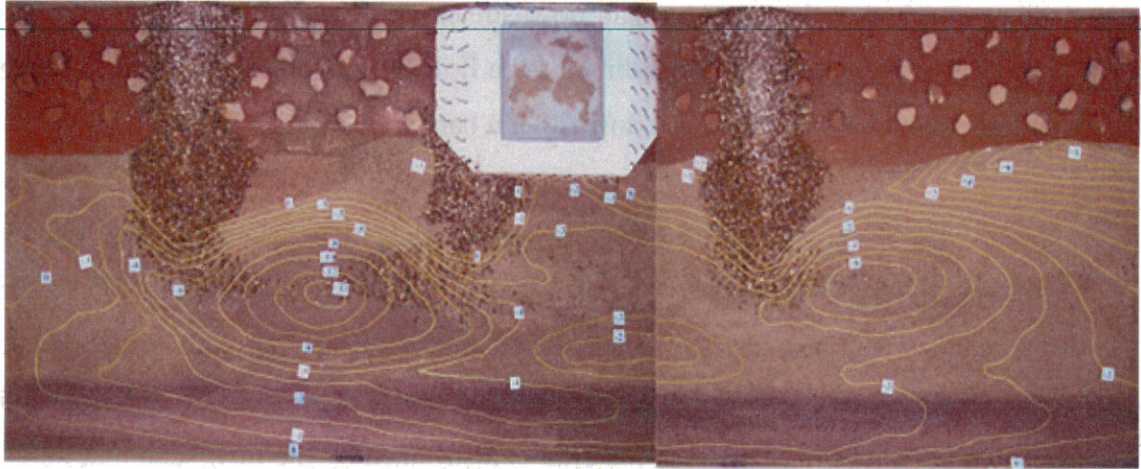


Fig. 7-8: Scour contour of Test Sp-9 with three spur dikes (including the one formed by the abutment). The flow was from left to right.

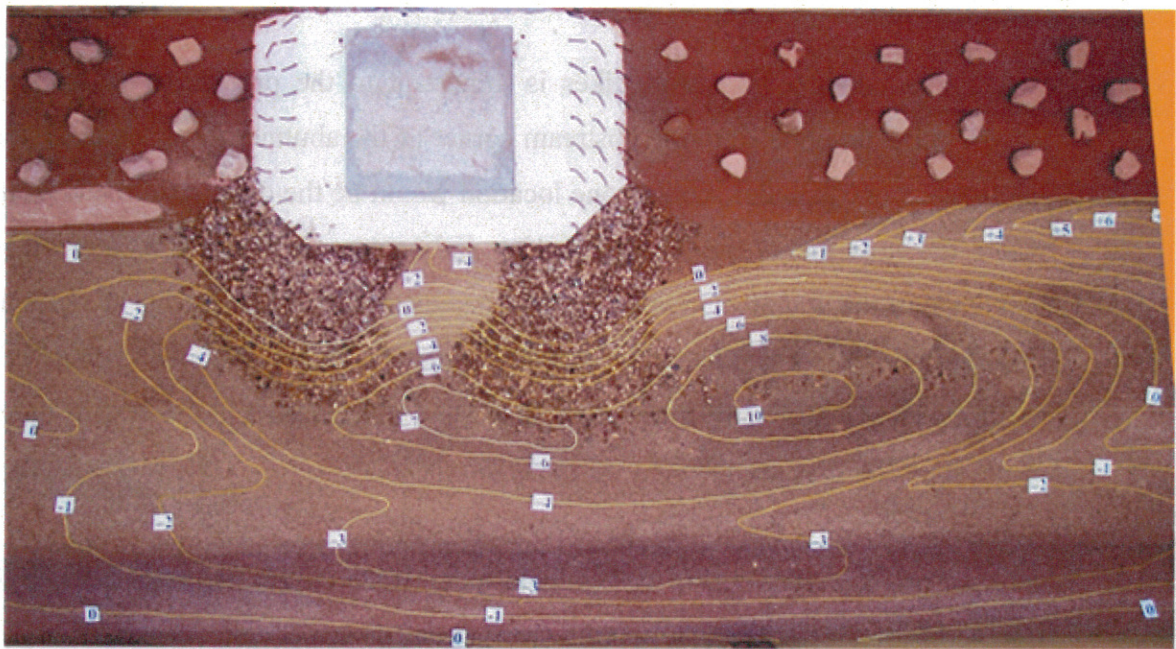


Fig. 7-9: Scour contour of Test Sp-10 with two spur dikes (both are located at the abutment). The flow was from left to right.

Generally the larger the number of spur dikes, the better the abutment will be protected, but at a higher cost. To minimize the cost, the number of spur dikes should be minimized. With this in mind, Sp-10 (Fig. 7-9) was performed with only two end-slope spur

configuration as Test Sp-11 except that there was initially a semicircular ring-shaped apron around each of the spur dike ends. Each apron had a width of about 20 cm and was about 3 rock diameters thick. Test Sp-13 and Test Sp-14 had similar spur dike configurations as Test Sp-10 except the aprons and rock size varied. There were similar aprons around the first two spur dikes in the later cases. In these cases, the flow depths were the same as for the clear water experiments. The velocity ratios (U/U_c) used were 1.5 and 2.3. The rock sizes used for the velocity ratio of 1.5 were of 19 ~ 50 mm in diameter and for the 2.3 velocity ratio were 50 ~ 70 cm in diameter. The top of each spur dike was approximately the same height as the top of the abutment. The live-bed experimental data are listed in Table 7-3.

Table 7-3: Live-bed experimental data of rock spur dikes ($Q = 0.0627 \pm 0.003 \text{ m}^3/\text{s}$ for velocity ratio of 1.5 and 0.0985 for velocity ratio of 2.3, $y_m = 13.2 \text{ cm}$, $y_f = 5.2 \text{ cm}$, running time $t = 3000 \text{ min}$).

Run No.	U/U_c	$d_{\text{abut.avg}}$ (cm)	$\%_{\text{max.abut.avg}}$	$d_{\text{max.sp1.avg}}$ (cm)	$d_{\text{max.sp1.inst}}$ (cm)	$d_{\text{max.sp2.avg}}$ (cm)	$d_{\text{max.sp2.inst}}$ (cm)
Sp-11 (Fig. 7-10)	1.5	-1.03*	114	5.11	10.35	4.92	9.93
Sp-12	1.5	-1.42	120	4.45	9.51	5.03	7.49
Sp-13 (Fig. 7-11)	1.5	-2.66	136	5.39	8.90	4.68	7.74
Sp-14 (Fig. 7-12)	2.3	-0.03	100	6.97	10.94	--	--

* Negative scour depths indicate deposition. $d_{\text{abut.avg}}$ = Time averaged scour depth at abutment; $\%_{\text{max.abut}}$ = Percent of scour reduction; $d_{\text{max.sp1.avg}}$ = Time-averaged scour depth in front of the 1st spur dike; $d_{\text{max.sp1.inst}}$ = Maximum instantaneous scour depth in front of the 1st spur dike; $d_{\text{max.sp2.avg}}$ = Time-averaged scour depth at the 2nd spur dike; $d_{\text{max.sp2.inst}}$ = instantaneous scour depth at the 2nd spur dike.

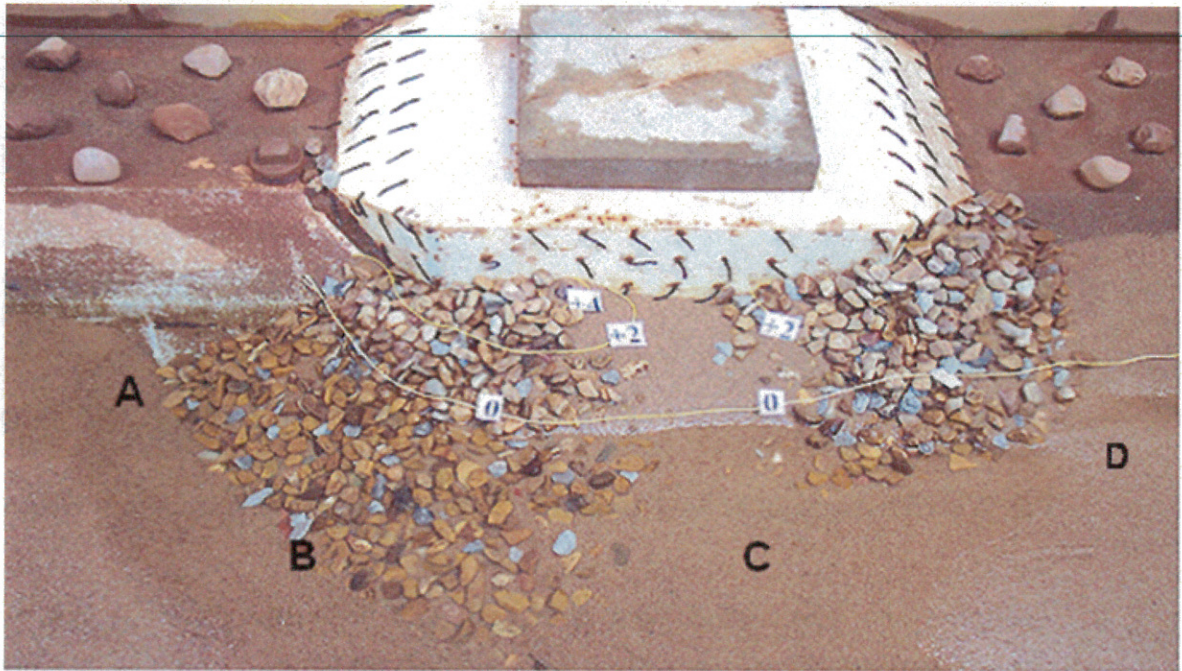


Fig. 7-10: Photograph of Test Sp-11 with two spurs attached at both ends of the abutment. Flow from left to right.

Although the configuration in Test Sp-11 and Sp-12 can protect the bed around the abutment, there is a concern about the portion of the floodplain at the upstream corner of the abutment. For erodible floodplains the spur dikes thus placed are not able to protect the floodplain. Compared to Test Sp-11 and Sp-12, data in both Table 7-3 and Fig. 7-11 showed that the configuration of Test Sp-13 can protect not only the channel bed around the abutment but also the floodplain and the abutment fill. The minimum deposition of sediment around the abutment was found to be 2.66 cm. Also because of the protection of the first spur dike, the spur dikes at both corners of the abutment experienced very little subsidence.

can launch aprons around the structure edges as the scour holes develop and prevent them from failing. Second, a sloped end at the main channel end of a spur dike whose top protrusion length is L will provide extra protrusion length and more deflection. Third, rock spur dikes may make deposition at the upstream of the abutment possible. The reason that the sediment did not deposit at the upstream corner of the abutment can be attributed to the fact that the abutment structure had a very smooth surface, and the flow velocity near the abutment surface was relatively high. This unimpeded velocity prevents settling of sediment. To conquer this problem, a pile of gravel placed at the upstream increases the roughness of the abutment and decreases the flow velocity so that sediment can deposit at the upstream corner of the piled rocks. Fourth, upward sloping rock spur dikes with relatively high friction roughness slow and guide the flow to climb up the slope instead of producing the scour-inducing downflow.

7.4 Design of Spur Dikes for Scour Prevention at Wing-wall Abutments

From the experimental results, it was concluded that spur dikes with top protrusion length of $1L$ and bottom length of $1.5L$ were sufficiently long to provide protection to the bridge abutment. The amount of material in the spur dikes can be greatly reduced if they are attached at the face of the abutment. The top length $1L$ is believed to be the minimum length required to protect the abutment while the bottom length is designed as a function of the rock's angle of repose. It was concluded for straight channels that the best spacing between successive spur dikes was $1L$. A spacing of $1L$ or less was able to restrict the flow from full separation behind each spur dike. As a consequence the scour depth behind each spur dike was less and the scour hole was pushed farther away from the spur dike end into the main channel.

It was concluded that 3 spur dikes, with the first one located $1L$ distance upstream of the upstream abutment corner, and the remaining two attached at the upstream and downstream corners of the abutment, respectively, would be the best configuration for preventing scour of the bed near the abutment for this experimental setup (stream-wise width of abutment is around L). For a bridge abutment whose stream-wise width is longer than $1L$,

protection to the abutment under the velocity ratios (U/U_c) of 0.9, 1.5, and 2.3. Two spur dikes at the upstream and downstream corners of the abutment were also successful at preventing scour in both clear-water and live-bed experiments.

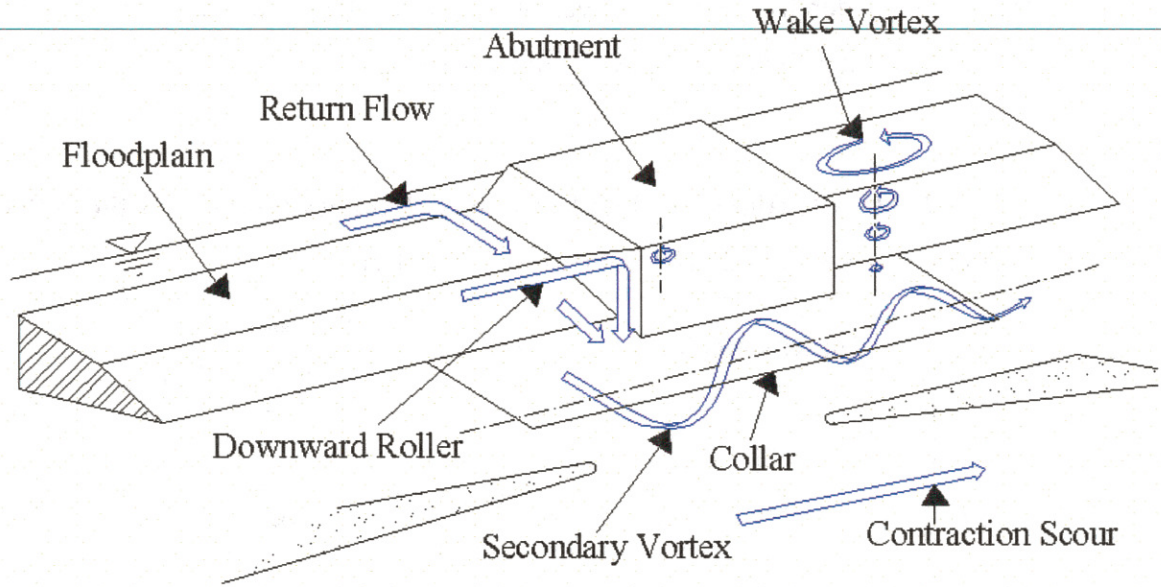


Figure 8-1: A sketch of the conceptual model of a collar as a countermeasure against abutment scour in a compound channel.

8.3 Collar Results

A series of collars of different lengths and widths were attached to the bridge abutment under clear-water conditions as countermeasures against scour at the abutment. These collars were made from steel and were seated horizontally at the desired elevation. The flow depth on the floodplain, y_f , was equal to 5.2 cm and the flow depth in the main channel, y_m , was 13.2 cm. The velocity ratio, U/U_c was 0.9 at the center of the entire channel as in the baseline tests. Table 2 gives the dimensions of each collar configuration tested.

Table 8-1 gives the results of the scour experiments with collars. Fig. 8-2 shows scour contours for equilibrium condition for Test T3. It was found that the collars were able to protect the bridge abutment efficiently by isolating the return flow and the secondary vortices from the bed around the abutment that ordinarily would cause local scour. The minimum collar dimensions that eliminated local scour were those with a width of $0.23L$ (L is the abutment length perpendicular to the flow direction) for elimination of local scour, a width of $0.8L$ for maximum reduction of scour at the edge of the collar, and having the collar located at a vertical location of $0.08y_m$ below the mean bed sediment elevation (y_m is the main

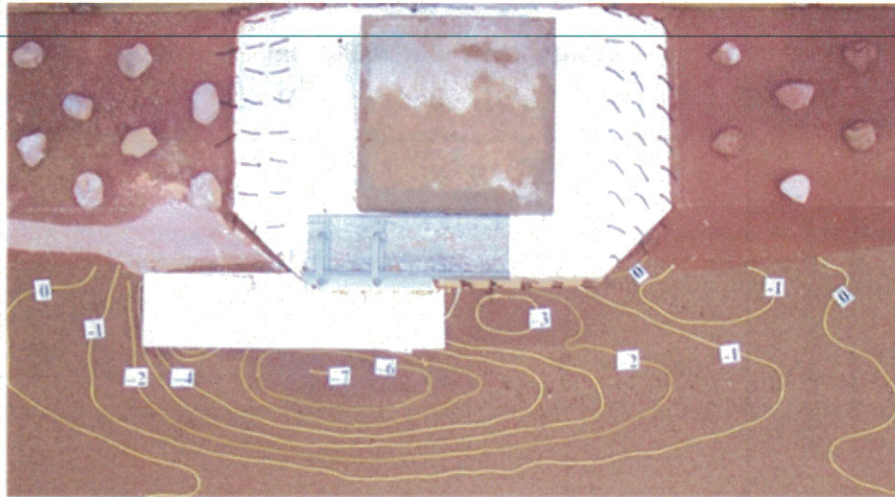


Figure 8-2: Elevation contours of Test T3 with collar at 1 cm below bed elevation. Flow from left to right. (See Table 8-1).

8.4 Discussion

8.4.1 Protrusion Width

Figure 8-3 is a plot of the maximum scour depth at both the bridge abutment and at the main channel edge of the collar versus the transverse collar width for all collar cases when the collar elevation was 1 cm below the initial bed level. It can be seen from Figure 8-2 that the maximum local scour depth under the main channel edge of the collar decreased from 7.10 cm to 1.00 cm as the width of the collar beyond the abutment increased from 10 cm to 35 cm.

Further examination of the experimental results shows that the maximum local scour depths at the main channel edge of each of these collars had a similar magnitude as the scour depth at the same location in the baseline case with no countermeasures. Figure 8-4 is a plot of the transverse bed profile in the bridge crossing of the baseline case and the scour profile formed by the maximum local scour depth values under the edge of the various collars of different widths. Fig. 8-4 suggests that the presence of the collar did

not change the strength of the vortex, but protected the abutment from scour by not allowing the scour-inducing secondary vortex to interact with the bed sediment.

8.4.2 Collar Elevation

To determine the optimal collar elevation, three different elevations of the collars were used in the experiments. Figure 8-5 shows the scour depth at the abutment and at the edge of the collars versus collar elevation for collars with a width of 10 cm. It is evident that an elevation of 1 cm below the original bed level had the least scour. This corresponds to an elevation of $1/13.2=0.08y_m$, where y_m is the flow depth in the main channel. The collar should be lower than the bed in order to keep the secondary vortex above it and not interacting with the bed sediment.

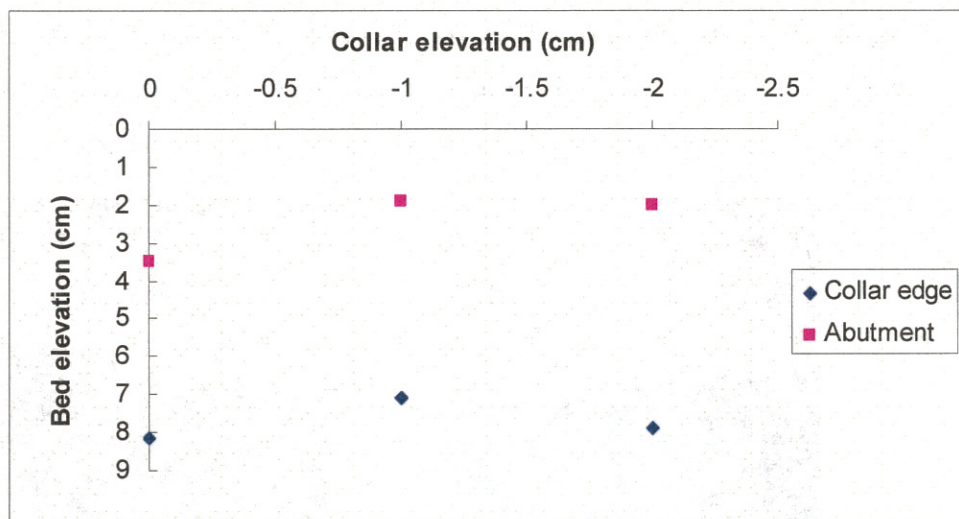


Figure 8-5: Plot of the bed elevation at the abutment and at the edge of the collars versus collar elevation. (All collars had a transverse width of 10 cm from the abutment face).

8.4.3 Streamwise Collar Length

At the upstream edge of the collar a shallow scour hole perpendicular to the flow was found in Tests T2 ~T4. This scour hole started from the main channel bank and went transversely towards the opposite channel wall and was connected to the scour hole at the

8.4.4 Temporal Scour Variation

It was observed that, unlike the rapid scour at the upstream and downstream abutment corners in the baseline case, the scour in the first ten hours under the main channel edge of the collar was very slow in all collar cases. Figure 8-7 is a plot of the temporal evolution of scour under the edge of the plate in Test T3. This delayed scour constitutes another advantage of using the abutment collars.

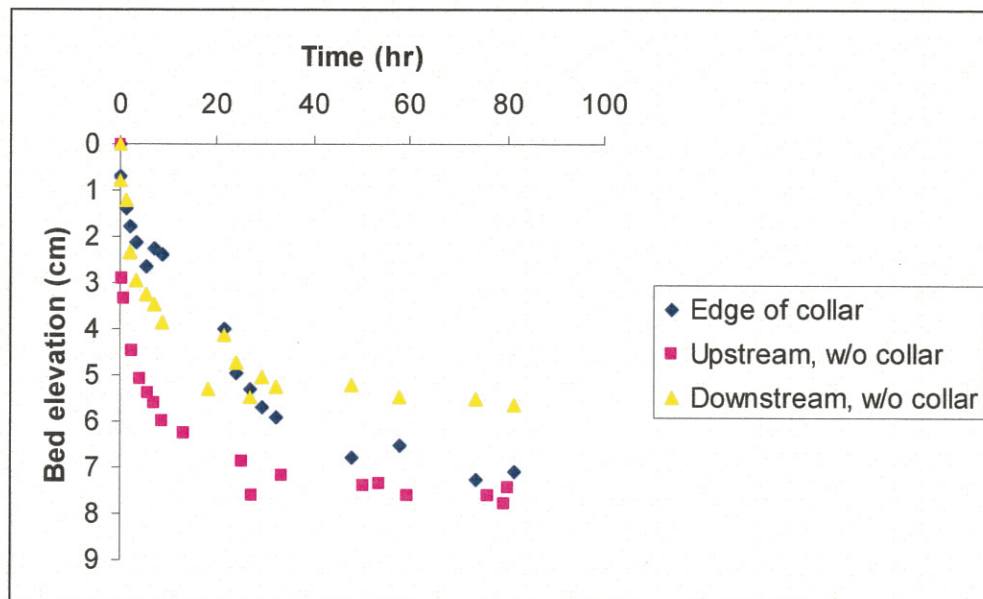


Figure 8-7: Plot of the scour depth variation under the main channel edge of the collar and for both the upstream and downstream scour holes versus time in Test T3. Note delayed scour in first 10 hours by collars.

8.5 Conclusions

From these clear-water experimental data, it can be concluded that:

1. Collars were found to be effective at preventing local scour at vertical wall bridge abutments. The collars isolated the turbulent flow and vortex systems from the bed material and therefore prevented the bed underneath the collar from scouring.
2. The further the collar extended downstream of the abutment, the farther downstream the scour hole was located. As the transverse width of the collars increased, the

CHAPTER 9. SUMMARY

9.1 Summary

Scour at bridge abutments can cause damage or failure of bridges and result in excessive repairs, loss of accessibility, or even death. To mitigate abutment scour, both clear-water and live-bed laboratory experiments in a compound channel were performed using parallel walls and spur dikes. In addition, collars were also tested under clear-water conditions only.

Two types of parallel walls were tested: the first type was made of a wood plate and the second was made of piled rocks. For solid parallel walls, a series of rectangular straight plates of different length attached to the upstream end of a wing wall abutment parallel to the flow direction were employed. The velocity of the flow for the three cases was either 0.9, 1.5 or 2.3 times the incipient motion velocity for bed sediment movement. The bed material was sand with a mean diameter of 0.8 mm and a standard deviation of 1.37. All the plates were seated at the bottom of the compound channel bank slope and were even with the abutment face.

It was found that straight plates thus situated caused the scour hole to be shifted away from the upstream corner of the abutment and to be effective as a countermeasure to prevent scour there. As the length of the plate increased, the scour at the abutment declined. It was found that a length of 1.6L, with L being the length of the abutment perpendicular to the flow, caused the scour to be eliminated at the abutment for a velocity ratio (U/U_c) of 0.9 (clear-water scour). Similarly, a 1.6L long wall can eliminate the time-averaged scour depth at the abutment 100 percent for a velocity ratio of 1.5, and 70 percent for a velocity ratio of 2.3. If the upstream end of the wall is anchored below the scour depth, this countermeasure can be feasible for situations where rock is expensive.

For parallel rock walls, various values of wall length and protrusion length into the main channel were tested. It was found that a wall that does not protrude into the main

length of equal or more than $1.9L$ could be tested further. The rigid floodplain could also be a limitation because in the real situations floodplains are generally erodible. The results here assume that the channel embankment does not erode. This corresponds to the case of cohesive channel banks, which is not uncommon. However, this should not have a major effect since the safety of the walls is not dependent on the floodplain. Since these results were obtained from the experiments at a greatly reduced scale, extrapolating to full-scale conditions could cause distortions. The velocity ratio (U/U_c), a commonly used similarity control variable in all hydraulic experiments balancing the hydraulic forces with the sediment resisting forces, was used to control the similarity of the experiments. In addition, bed forms typical of natural rivers were observed throughout the experiments. This does not guarantee, however, that there will not be differences between the laboratory and field results due to differences in scaling of the turbulent eddies and vortices formed. Scour produced at a small scale is usually more severe than that in the field, however, making the results of the lab study conservative.

9.3 Future Work

The design guidelines offered here for each countermeasure are developed under limited laboratory conditions. More work can follow after this study. For instance, it would be necessary to test the effect of roughness on the floodplain on the scour depth at the abutment. Channel setup with erodible floodplain, non-uniform sediments will make the experiments more realistic. Different abutment orientations, length, shapes, and configurations with higher flow velocity ratios can be tested.

Effect of permeability of rock structures on their own stability and protection efficiencies can be studied. Collars as countermeasures against abutment scour under live-bed conditions are difficult to test since it is hard to monitor and measure the scour depth under the collar around the abutment. However, it should be tested for the integrity of the study. Also, methods of how to attach a collar to a bridge abutment should also be studied to make this collar as practical as other countermeasures.

REFERENCES

- Acheson, A. R. (1968). "River control and drainage in New Zealand and some comparisons with overseas practices." Ministry of Works, New Zealand, 296 pp.
- Ahmad, M. (1951). "Spacing and projection of spurs for bank protection." Civil Engineering and Public Work Review, London, U. K. March 172-174, April 256-258.
- Ahmad, M. (1953). Experiments on design and behavior of spur dikes. Proceedings, Minnesota International Hydraulics Convention, International Association of Hydraulic Research, Minneapolis, Minnesota.
- Ahmed, F. and Rajaratnam, N. (2000). "Observations on flow around an abutment." J of Engineering Mechanics, ASCE, Vol. 125, No. 1, pp. 51-59.
- Baker, R.E. (1986). "Local scour at bridge piers in nonuniform sediments." School of Engineering Report, no. 402, University of Auckland.
- Blench, T. (1969). Mobile-Bed Fluviology. University of Alberta Press, Edmonton, Alberta, Canada.
- Bradley, J.N. (1978). "Hydraulics of Bridge Waterways." Hydraulic Design Series No. 1, U.S. Dept. Transportation, Federal Highway Administration, 2nd Ed., Washington, D.C.
- Brice, J.C. and Blodgett, J.C. (1978). "Countermeasures for hydraulic problems at bridges." Volume I and II, Federal Highway Administration, Report FHWA-RD-78-162 and Report FHWA-RD-78-163.
- Brown, S. A. (1985). Design of spur-type stream bank stabilization structures, Final Report. FHWA/RD-84-101, Federal Highway Administration, Washington, D. C.
- Brown, S.A. and Clyde, E.S. (1989) "Design of riprap revetment," Hydraulic Engineering Circular 11 (HEC-11), Report No. FHWA-IP-89-016, Federal Highway Administration, U.S. Department of Transportation, Washington, D.C., U.S.A.
- Cardoso, A. H. and Bettess, R., (1999) "Effects of Time Channel Geometry on Scour at Bridge Abutments." Journal of Hydraulic Engineering, vol. 125, issue 4 pg. 388-399
- Central Board of Irrigation and Power (1989) "River behavior management and training," edited by C.V.J. Sharma, K.R. Saxema and M.K. Rao, Publication No. 204, Vol. 1, Central Board of Irrigation and Power, New Delhi, India, 469pp.

- Franzetti, S., Larcán, E., Mignosa, P. (1982) "Influence of test duration on the evaluation of ultimate scour around circular piers." Proc. Int. Conf. Hydraulics and Modelling of Civil Structures, Coventry, England, pp 381–396.
- Froehlich, D. C. (1989). "Local Scour at Bridge Abutments", proceedings of the 1989 National Conference on Hydraulic Engineering, Edited by Michael A. Ports, New Orleans, Louisiana.
- Gales, R.R. (1938). "The principles of river training for railway bridges, and their application to the case of the Harding Bridge over the Lower Ganges at Sara." J. Inst. of Civil Engrs (UK), 10(2), p.136.
- Garde, R. J., Subramanya, K., Nambudripad, K. D. (1961). Study of scour around spur dikes. ASCE Journal of the Hydraulics Division, 87(HY6), 23-37.
- Gill, M. A., (1970) "Bed erosion around obstructions in rivers." Ph.D thesis, The University of London (Imperial College of Science and Technology).
- Gill, M. A. (1972). "Erosion of sand beds around spur dikes." Journal of the Hydraulics Division, 98(HY9), 1587-1602.
- Grant, A. P. (1948). Channel improvements in alluvial streams. Proceedings, New Zealand Institution of Engineers, Vol. XXXIV, p. 231-279.
- Hagerty, D.J. and Parola, A.C. (1992). "Seepage influence on stability of bridge abutments." Conf. Proc. Hydraulic Engrng, 1992, ASCE, p. 900.
- Herbich, J. B. (1967). "Prevention of Scour at Bridge Abutment. International Association for Hydraulic Research." Proceedings of the Twelfth Congress of the International Association for Hydraulic Research, Sept. 11-14, 1967.
- Inglis, C. C. (1949). The behavior and control of rivers and canals. Research Publication No. 13, Parts I and II, Central Waterpower Irrigation and Navigation Research Station, Poona, India.
- Izzard and Bradley (1957) "Field verification of model tests on flow through highway bridges and culverts." Proceedings, 7th Hydraulic Conference, Iowa.
- Jansen, P. Ph., ed. 1979. Principles of River Engineering, Pitman, London, England.
- Johnson, P.A. (1994). "Quantification of bridge pier scour uncertainty." Machine Intelligence and Pattern Recognition, Vol. 17, pp. 407.

- Kuhnle, R. A.; Alonso, C.V., Shields, F.D. (1998). "Volume of scour holes for angled spur dikes." Proc. 1998 Int. Water Resources Engrg Conf. Part 2 (of 2) v 2 1998, ASCE, p .1613.
- Kuhnle, R. A.; Alonso, C.V., Shields, F.D. (1999). "Geometry of scour holes associated with 90-degree spur dikes." J. Hydraulic Engrg v 125 n 9 Sep, 1999, ASCE, p.972.
- Kwan, F., (1984). "Study of Abutment Scour", Report No. 328, University of Auckland, School of T. Engineering, Department of Civil Engineering Private Bag, Auckland, New Zealand.
- Kwan, F., (1987) "A study of abutment scour." PhD thesis, University of Auckland.
- Kwan, F., (1988). "Study of Abutment Scour", Report No. 451, University of Auckland, School of T. Engineering, Department of Civil Engineering Private Bag, Auckland, New Zealand.
- Lagasse, P.F, Schall, J.D., Johnson, F., Richardson E.V., and Chang, F. (1995) "Stream Stability at Highway Structures." Report No. FHWA IP-90-014, HEC-20, FHWA.
- Lagasse P. F., Richardson E. V., and Zevenbergen L. W. (1996). "Design of Guide Banks for Bridge Abutment Protection". North American Water and Environment Congress & Destructive Water. Conference Proceeding, *New York: ASCE*, 0-7844-0166-7 pp. 4188-4197.
- Lagasse, P.F., Byars, M.S., Zevenbergen, L.W., and Clopper, P.E. (1997). "Bridge scour and stream instability countermeasures." FHWA HI-97-030 HEC-23, FHWA.
- Lagasse P. F., Richardson E. V., and Zevenbergen L. W. (1999). "Design of Guide Banks for Bridge Abutment Protection." Stream Stability and Scour at Highway Bridges. *Reston, VA: ASCE*, 0-7844-0407-0, pg. 856.
- Lagasse, P. F., Zevenbergen, L. W., Schall, J. D., Clopper, P. E. (2001). "Bridge Scour and Stream Instability Countermeasures." Publication No. FHWA NHI 01-003, Hydraulic Engineering Circular No. 23, U. S. Department of Transportation, Federal Highway Administration. Pages 2.7, 2.9, 4.6, 6.16 - 6.18, Design Guidelines 1, 9, 10.
- Lauchlan, C.S. and Melville, B.W. (2001) "Riprap protection at bridge piers," Journal of Hydraulic Engineering, v 127, n 5, May, 2001, p 412-418
- Laursen, E.M. (1952). "Observation on the nature of scour." Proceedings, 5th Hydraulics Conference, Iowa.

- Melville, B.W., (1975). "Local scour at bridge sites." School of Engineering, Report No. 117, University of Auckland.
- Melville, B.W. and Sutherland, A.J., (1988). "Design method for local scour at bridge piers." ASCE, Journal of Hydraulic Engineering, Vol. 114, No. 10, pp. 1210-1226.
- Melville, B.W. (1992). "Local Scour at Bridge Abutments." ASCE Journal of Hydraulic Engineering, Vol. 118, No. 4, April, 1992, pp. 615.
- Melville, B.W. (1995). "Bridge abutment scour in compound channels." J. Hydr., Engrg., ASCE, 121(12), p. 863.
- Melville, B. W. (1997). Pier and abutment scour: integrated approach. Journal Hydraulic Engineering, 123(2), 125-136.
- Melville, B.W. and Coleman, S.E. (2000). Bridge Scour, Water Resources Publications.
- Ministry of Works and Development (1979). "Code of practice for the design of bridge waterways." Civil Division Publication CDP 705/C, Ministry of Works and Development, Wellington, New Zealand, 57pp.
- Miller, M. C., McCave, I. N., Komar, P. D. (1977). "Threshold of sediment motion under unidirectional currents." Sedimentology, v. 24, p. 507-527.
- Molinas, A., Kheireldin, K., Wu, and Baosheng (1998). "Shear stress around vertical wall abutments." J. Hydraulic Engrg, v 124 n 8 Aug 1998 ASCE, p.822.
- Mueller, D.S. and M.N. Landers, 1999, "Portable Instrumentation for Real-Time Measurement of Scour at Bridges," Federal Highway Administration Publication No. FHWA-RD-99-085 (FHWA approval pending), Turner-Fairbank Highway Research Center, McLean, VA.
- Muneta and Shimizu, 1994 "Numerical analysis model with spur-dike considering the vertical flow velocity distribution" Proc. Japan Soc. of Civil Engrg n 497 pt 2-2 1994 p. 31.
- Neill, C.R. (1973). "Guide to bridge hydraulics." Roads and Transportation Assoc. of Canada, Univ. of Toronto Press, Toronto, Canada.
- Odgaard, A.J. and Wang, Y. (1991). "Sediment management with submerged vanes. II: Applications." Journal of Hydraulic Engineering, v 117, n 3, Mar, 1991, p 284-302.
- Oliveto, G, Hager, W. H., (2002) "Temporal evolution of clear-water pier and abutment scour." J. Hydraul. Eng., Am. Soc. Civ. Eng. 128: 811-820

- Richardson, E.V. and Davis, S.R. (1995) "Evaluating scour at bridges," Report No. FHWA-IP-90-017, Hydraulic Engineering Circular No. 18 (HEC-18), Third Edition, Office of Technology Applications, HTA-22, Federal Highway Administration, U.S. Department of Transportation, Washington, D.C., U.S.A., November, 204pp.
- Richardson, E. V., Lagasse, P. F., eds. (1999). Stream Stability and Scour at Highway Bridges, Compendium of Papers ASCE Water Resources Engineering Conferences 1991 to 1998.
- Richardson, E. V., Simons, D. B., Lagasse, P. F. (2001). Highways in the River Environment. Report No. FHWA NHI 01-004, Hydraulic Design Series No. 6, Federal Highway Administration, Washington, D. C.
- Richardson and Richardson (1993a), "The fallacy of local abutment scour equations." Conf. Proc. Hydraulic Engng, 1993, ASCE, p. 749.
- Richardson, J.R. and Richardson, E.V. (1993b) "Determining contraction scour." Stream Stability and Scour at Highway Bridges, ASCE Reston, VA pp. 483-91.
- Richardson, J.R. and York, K. (1999). "Hydrodynamic countermeasures for local pier scour." Transportation Research Record n1690 1999 p 186.
- Sastry, C. L. N., (1962) "Effect of spur-dike inclination on scour characteristics." M E thesis, University of Roorkee, Roorkee.
- Sellin, R.J.H., (1964). "A laboratory investigation into the interaction between the flow in a channel of a river and that over its floodplain." La Houille Blanche, 19(7), 793-807
- Shields, F. D., Jr., Cooper, C. M., and Knight, S. S. (1995). Experiment in stream restoration. Journal of Hydraulic Engineering, 121(6): 494-502.
- Simons, D.B. and Lewis, G.L. (1971) "Report - flood protection at bridge crossings," prepared for the Wyoming State Highway Department in conjunction with the U.S. Department of Transportation, C.S.U. Civil Engineering Report No. CER71-72DBS-GL10.
- Smith, C. D. (1984). "Scour Control at Outlook Bridge---a Case Study. " Canadian Journal of Civil Engineering, v 11, n 4, Dec, 1984, p 709-716 ISSN: 0315-1468.
- Soliman, M.M., Attia, K.M., Kotb, Talaat, A.M., and Ahmed, A.F."Spur dike effects on the river Nile morphology after high Aswan dam." Proc., Cong. Int. Assoc. Hydraulic Research, Part v A 1997 p 805.

- Thomas Molls; Chaudhry, M. Hanif; Khan, K. Wasey (1995) "Numerical simulation of two-dimensional flow near a spur-dike." *Advances in Water Resources* v18 n4 1995 p. 227.
- Tingsanchali, T. and Maheswaran, S. (1990). "2-D Depth Averaged Flow Computation Near a Groyne." *Journal of Hydraulic Engineering, ASCE, New York, U.S.A., January, Vol. 116, No. 1, pp. 71-86.*
- Tison, G. 1962. "Discussion of "Study of Scour around Spur Dikes," *Journal, Hydraulics Division, ASCE, Vol 88, No. HY4, pp 301-306.*
- .Tominaga, A., Nagao, M., and Nezu, I (1997). "Flow structures and mixing processes around porous and submerged spur dikes." *Proc. 27th Congress of the Int. Assoc. of Hydraulic Resrch., IAHR. Part B-1 v B pt 1 p 251.*
- United Nations Economic Commission for Asia and the Far East. (1953). *River Training and Bank Protection. Flood Control Series no. 4, Bangkok.*
- U. S. Army Corps of Engineers, 1978. "Minutes of the Symposium on Design of Groins and Dikes," held at the U. S. Army Waterways Experiment Station, CE, Vicksburg, Miss..
- White, F.M. (1974) *Viscous Fluid Flow, McGraw-Hill.*
- Whitehouse, R.J.S. (1997) "Scour at marine structures: a manual for engineers and scientists." *Res. Rep. R417, HR Wallingford Limited, Wallingford, UK.*
- Wong, W. H. (1982). "Scour at Bridge Abutments". Report No. 275, Dept. of Civil Engineering, University of Auckland, Auckland, New Zealand.
- Wu, X.; Lim, S.Y (1993). "Prediction of maximum scour depth at spur dikes with adaptive neural networks." *Civil-Comp93, Part 3: Neural Networks and Combinatorial Optimization in Civil and Structural Engineering Civil-Comp93, p 61.*
- Zaghloul N. and McCorquodale J. A. MCSCE (1973) "A numerical model for flow past a spur-dike" *Proceedings of the First Canadian Hydraulics Conference, May 10 & 11, Edmonton, Canada, p355-368.*
- Zaghloul, N.A. and McCorquodale J.A., (1975) "A stable numerical model for local scour." *I.A.H.R. Journal of Hydraulic Research, Vol. 13, No. 4.*
- Zaghloul N. A. (1983). "Local scour around spur-dikes." *Journal of Hydrology, 60 (1983) 123-140.*
- Zhang, Y. and Du, X., (1997). "Limited scour around spur dike and the evaluation of its depth." *J. Xi'an Highway Transportation University v17 n4 97 p 56.*